EFFECTS OF BORONIZING ON GROOVED METAL SURFACE

JOHNNIE LIEW ZHONG LI

UNIVERSITI TEKNIKAL MALAYSIA MELAKA

EFFECTS OF BORONIZING ON GROOVED METAL SURFACE

JOHNNIE LIEW ZHONG LI

A report submitted
in fulfillment of the requirement for the degree of
Bachelor of Mechanical Engineering (Structure and Material)

Faculty of Mechanical Engineering

UNIVERSITI TEKNIKAL MALAYSIA MELAKA

2017

DECLARATION

I declare that this report entitle "The effect of boronizing on grooved metal surface" is the result of my own research except as cited in the references.

Signature : ....

Name of Student : ……………………………..

Date : ………………………………..

SUPERVISOR'S DECLARATION

I have checked this report and the report can now be submitted to JK-PSM to be delivered back to supervisor and to the 2nd examiner.

Signature	: …………………………
Name of Supervisor	: …………………………
Date	: ………………………....

DEDICATION

To my beloved father and mother

ABSTRACT

The main purpose of this project was to study the effects of temperature and time on the boride layer thickness of grooved surface. Boronizing is a thermo-chemical surface hardening process that allow the boron atoms diffuse into the metal surface. Different geometry groove surface is expected to affect the boronizing thickness and diffusion rate. The boronizing thickness and effectiveness of diffusion rate on different grooved geometry surfaces were studied. There were nine fabricated specimens in this project. Each of the specimen has four different grooved surfaces which are U-shaped (rectangular), 2mm C-shaped (circular), 4mm C-shaped (circular) and V-shaped (triangular). The specimens were placed in furnace for heating process. The boronizing time were 2 hours, 4 hours and 6 hours wheareas the boronizing temprature were 1123K, 1173K and 1223K. The specimens were cooled down in room temperature. Specimens were grinded and polished. The specimens were characterized for boride layer thickness measurement by using Scanning Electron Microscope and Inverted Optical Microscope. The activation energy of each grooved surface was calculated and analysed. The result and analysis showed that the boronizing thickness of different geometry surfaces were increased with temperature but inconsistent with time.

ABSTRAK

Tujuan utama projek ini dijalankan adalah untuk mengkaji bagaimana suhu dan masa mempengaruhi ketebalan lapisan borida pada permukaan beralur. Penyusukanboronan adalah satu proses pengerasan permukaan termo-kimia yang membolehkan atom boron meresap ke dalam permukaan logam. Perbezaan permukaan geometri alur dijangka memberi kesan kepada ketebalan dan kadar resapan penyusukboronan. Ketebalan penyusukboronan dan keberkesanan kadar resapan pada permukaan geometri beralur yang berbeza telah dikaji. Sembilan spesimen telah disediakan dalam projek ini. Setiap spesimen mempunyai empat permukaan beralur yang berbeza bentuk iaitu; bentuk-U (segi empat), bentuk-C bersaiz 2mm (bulat), bentuk-C bersaiz 4mm (bulat) dan bentuk-V (segi tiga). Semua spesimen telah diletakkan ke dalam dandang untuk proses pemanasan. Masa proses pemanasan adalah 2 jam, 4 jam dan 6 jam. Suhu proses pemanasan pula adalah 1123K, 1173K dan 1123K. Setiap spesimen telah disejukkan dalam suhu bilik. Pencirian spesimen telah dilakukan untuk pengukuran ketebalan lapisan borida dengan menggunakan alat Mikroskop Imbasan Electron dan Mikroskop Optik. Tenaga pengaktifan untuk setiap permukaan beralur telah dikira dan dianalisis. Keputusan dan analisis menunjukkan bahawa ketebalan penyusukboronan pada permukaan geometri yang berbeza telah meningkat dengan suhu tetapi tidak konsisten dengan masa.

ACKNOWLEDGEMENT

I would like to express my gratitude to my supervisor, Dr. Rafidah Binti Hassan, who has helped me so much by constantly imparting her knowledge and suggestion so that i could complete my PSM project successfully. Besides, sincere thanks to Dr. Mohd Zulkefli Bin Selamat and Dr. Siti Hajar Bt Sheikh for evaluating my final year project and presentation. The suggestions and ideas given were precious for me to finalized this PSM project.

In addition, i would like to thank Faculty of Mechanical Engineering (FKM), Universiti Teknikal Malaysia Melaka (UTeM) for giving me this chances to finish this project and allow me to utilize all the required equipment and machines for this project. Eventually, i would like to acknowledge with much appreciations to my family and friends for thier encouragement and supports throughout the project duration.

TABLE OF CONTENT

LIST OF TABLES

LIST OF FIGURES

LIST OF ABBEREVATIONS

CVD-5B	-	Chemical Vapor Diffusion process
CNC	-	Computer Numerical Control

LIST OF SYMBOLS

x	-	Thickness
K	-	growth rate constant
t	-	Time
Q	-	Activation energy
T	-	Temperature
x	-	Horizontal displacement
y	-	Vertical displacement
µm	-	Micrometer
UTeM	-	Universiti Teknikal Malaysia Melaka
HV	-	Hardness Vickey

LIST OF APPENDICES

CHAPTER 1

INTRODUCTION

1.1 BACKGROUND OF STUDY

There are numerous surface hardening technologies at the present time. Thermal spray (Sampath, 2015), stellite (Kapoor, 2012) and hard chromium plating (Koorapati *et al*., 2013) are methods that often used in metal hardening. Boronizing or so called boriding can achieve reliable effect in metal hardening process. Boronizing is a chemical vapor diffusion process (CVD-5B) which allow the boron atoms diffuse into the metal surface of a wide variety of ferrous and non-ferrous materials to form complex boride such as Iron Boride (FeB) and Iron(II) Boride (FeB_2) (Buijnsters *et al*., 2003). This process are surrounded by a boron rich substance such as a fine powder or granulated medium before being taken to elevated temperature for a time during which the boron diffuses into the outer layer of the steel. Chemical vapor diffusion frames a hard layer that attains a hardness of close to Rockwell Hardness of around 84 HRC and strong wear-resistant metal mesh on the metal surface (Black and Kohser, 2008).

Practically all the ferrous material can be boronized including titanium (Ti), Nickel (Ni) and Cobalt alloy (Co). Nevertheless, the content of alloy element has direct influence to the diffusion rate. Higher content of alloy element might have longer the diffusion rate. The boride layer thickness is varied according to temperature, treatment duration and material. Boride layer thickness is around 10μm-200μm and it can attain a Vickers Hardness of between 1600HV to 2000HV (Arun *et al*., 2013). Boron yielding material can be heated to temperatures between 650 ºC to 1000 ºC (1200ºF-1830ºF) during the boronizing process (CVD-5B). Thus, metal that undergo boronizing is immensely wear resistant and last longer than conventional heat treatment such as Nitriding, Carburizing and Nitrocarburizing (Suwattananont, 2004).

Boronizing include ferrous metals, non-ferrous metal and alloys as shown in Table 1.1. Different material has different properties and outcome. Boronizing increases the hardness of ferrous material and temperature resistance by 1400HV-2000HV and 1830ºF respectively (Jurci and Hudakova, 2010). Most importantly the boride layer can reduce the coefficient of friction and the resistance of acid. In addition, heat treatment can be fully hardened after boronizing. Treatment can apply to irregular shape and it dimension of diffusion layer are adjustable.

Table 1.1 Material of boronizing (Adapted from Fichtl, 1981)

Ferrous Metal	Non-Ferrous Metal	Alloy
• Stainless steel • Carbon steel • Wrought Iron • Mild steel • Cast iron	• Aluminum • Copper • Silver • Lead	• Hastelloy • Nimonic 80A • Inconel 625

1.2 PROBLEM STATEMENT

Steel is an important material that comprises many residential and commercial structures. It ranks among the sturdiest construction material and multi shaped. Different geometry on groove surface is expected to affect the boronizing thickness and diffusion rate. In this project, the boronizing thickness and the effectiveness of diffusion rate on different grooved geometry surfaces are studied.

1.3 OBJECTIVES

1. To identify how the temperature and time affect the boronizing thickness on the grooved surface by using metallographic analysis.
2. To analyses the effect of different grooved geometries on the boronizing diffusion by using activation energy analysis.

1.4 SCOPE OF PROJECT

The scopes of this study focus on:

1. The boronizing apparatus design, preparation and process.
2. The analysis of diffusion for boride layer thickness by using microscopic observation.
3. The analysis of activation energy for boronizing on different grooved geometry surfaces.

CHAPTER 2

LITERATURE REVIEW

2.1 BORONIZING

Boronizing is a thermo-chemical surface hardening process that enables the boron atom diffuse into a pedestal metal to create a compact metallic boride layer on the surface. Boron atom disperse into the metallic lattice of the metal surface by heating in the temperature range of 1200°F- 1830°F during the boronizing process (Suwattananont, 2004). As a consequence, a single-phase boride or poly-phase boride appear and form an interstitial boron compound. The boron compound layer is usually about 20µm-300µm. Different substrates have different microhardness and constituent phases of the boride layer as shown in Table 2.1. Thermo-chemical surface treatments can strengthen the resistance to corrosion and abrasive wear, decreases coefficient of friction and increase the surface hardness. Boronizing can be applied to ferrous metals, non-ferrous metals and alloys. Magnesium alloy and aluminium alloys cannot be boronized because of its low melting point.

Table 2.1: Constituent phase and microhardness of different substrate (Adapted from Suwattananont, 2004)

Substrate	Constituent phases in the boride layer	Microhardness of layer, HV
Fe	FeB Fe_2B	1900-2100 1800-2000
Co	CoB Co_2B	1850 1500-1600
Co-27.5 Cr	CoB Co_2B	2200 (100g) ~1550 (100g)
Ni	Ni_4B_3 Ni_2B Ni_3B	1600 1500 900
Inco 100	-	1700 (200g)
Mo	Mo_2B Mo_2B_5	1660 2400-2700
W	W_2B WB W_2B_5	~2700 (overall hardness)
Ti	TiB TiB_2	2500 3370
Ti-6Al-4V	TiB TiB_2	3000(100g)(overall hardness)
Nb	Nb_2B_2 NbB_4	2600-3000 (overall hardness)
Ta	Ta_2B TaB_2	3200-3500 2500
Zr	ZrB_2 Zr_2B	2300-2600 (overall hardness)
Re	ReB	2700-2900

2.1.1 Material of boronizing

Borides can be formed on ferrous metal, non-ferrous metal and alloys. There are two separate reactions during the process. The first reaction is a steady process between the boron merge with the base-metal surface and form a hard and thin boride layer. Second reaction is the boron atoms diffused further into the substrate at a faster rate and form a boron compound layer. (Keddam *et al*., 2015)

<u>Ferrous metal</u>

Most of the ferrous metals can be boronized such as low-alloy steel, tool steel, stainless steel, carbon steel, and mild steel. The boron compound layer will be formed on the ferrous metal surface. The boron compound layer can be either in single phase formation or double phase formation with a certain composition. The single phase consists of Fe_2B layer whereas the double phase formation consists of FeB layer and Fe_2B layer as shown in Figure 2.1. (Yorulmaz, 2007)

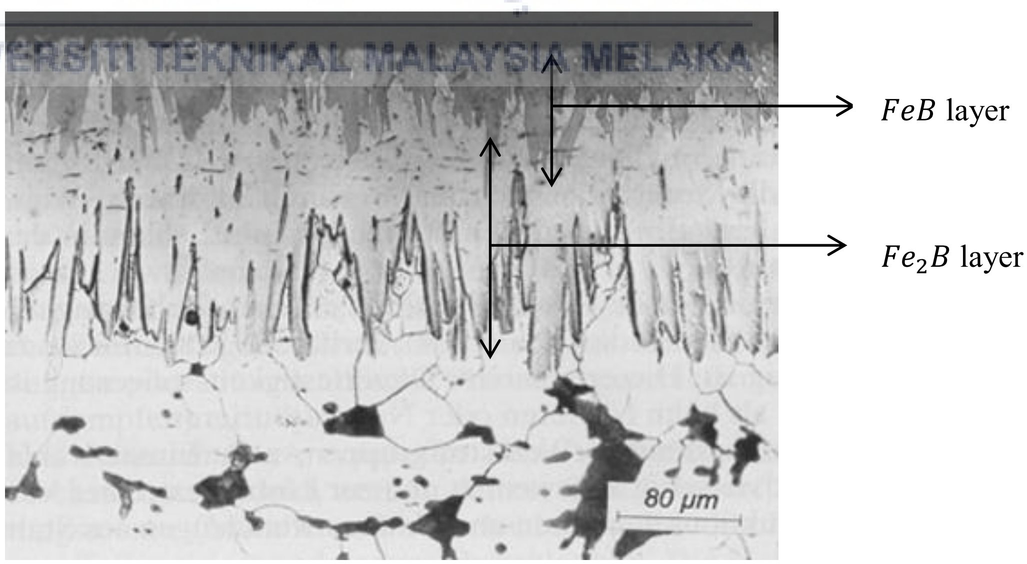

Figure 2.1: Boron compound layer consists of FeB layer (dark) and Fe_2B layer (light) (Krastev, 2012)

Non-ferrous metal

Titanium, cobalt, nickel and alloys are non-ferrous metal. These materials can be boronized by using thermo-chemical surface treatment process since the salt bath and conventional powder boronizing technique are inapplicable for refractory metals and titanium due to the oxidation on the substrate. Thus, the titanium and refractory heat treatment can only operate under high purity argon atmosphere and high vacuum. The heat treatment temperature for titanium and refractory metal are above 1000°C (>10 hours). The boride layer thickness is approximately 50μm and its microhardness is 2500HV-3370HV. (Suwattananont, 2004)

Alloy elements

Alloy elements can affect the morphology thickness and the character of the boronizing layer that formed on the steel surface (Tsipas and Rus, 1987). Alloy elements can refine the properties of boride layer by entering the boride coating and influence its lattice sites to form distinct particles inside the coating (Tsipas and Rus, 1987). Beside, alloy elements have great effect in the disposition of boride layers and create an isolated well-differentiated continuous boride layer. It is noted that alloy content is directly proportional to the diffusion rate of the boronizing (Fichtl, 1981). The difficulty of the boron atoms diffuse into steel will increase as the content of alloy increase.

2.1.2 Type of boronizing

Boronizing is a thermo-chemical surface treatment technique. They are a lot of method to diffuse the boron atoms on the surface of metal. These are six types of thermo-chemical surface treatment method which are pack boronizing, paste boronizing, liquid boronizing, gas boronizing, plasma boronizing and fluidized bed boronozing (Krastev, 2012). Unfortunately, there are only pack boronizing and paste boronizing have achieved commercial success due to its low procedure cost and high quality product that is filled up the gap between low and high technology. Beside, gas boronizing and liquid boronizing have limited application due to the environmental problem. This situation has increased the use of pack boronizing and paste boronizing as compared to gas boronizing, liquid boronizing and other boronizing method.

Pack boronizing is a process that boronize the metal by using boron powder mixture. Boron powder consist of ferroboron, amorphous boron (B_4C), fluxes and activators($NaBF_4, KBF_4$). Boron powder and metal are packed into a container and heated at 800°C to 1000°C for several hours to produce a boride layer on the metal surface (Yorulmaz, 2007). Paste boronizing is alike to pack boronizing but paste boronizing has lower cost and less difficulty compare to pack boronizing. Paste boronizing used B_4C as the boronizing agent, activator, fluxes and binding agent to perform paste formation. The heat temperature for paste boronizing is from 800°C to 1000°C and the process is heated inductively (Krastev, 2012).

Gas boronizing are quite similar to plasma boronizing. These method are hazardous due to its mixture used. Gas boronizing and plasma boronizing are carried out in $B_2C_6 - H_2$ or $BCI_2{-}H_2$ (Krastev, 2012). These mixtures have level of toxicity and explosively in gaseous atmosphere. These situations lead to gas boronizing and plasma boronizing to a condition of not achieving commercial acceptance even though plasma boronizing has advantage in boronize the metal in lower temperature.

Fluidized bed boronizing is carried out in a special retort furnace. The mixtures used are bed material of coarse silicon carbide particles, a special boride powder and oxygen-free gas atmosphere from nitrogen-hydrogen gas (Yorulmaz, 2007). This process has advantages in quantity, cost, time and energy consumption. Fluidized bed boronizing can be used in continuous production and low operation cost since the operating time is reduced. But this process still new in boronizing technologies and lack of research and testing evidences to evaluate it features.

2.1.3 Factor and reaction of boronizing

The thickness of boride layer is depends on the temperature and time of boronizing. The boride layer consists of three regions which are borides, transition zone and matrix (Topuz *et al.*, 2015). Boride layer thickness increased when the temperature and time of boronizing increase due to the boronizing kinetics which is a thermally activated phenomenon as shown in Figure 2.2. The boride layer can be either in single phase formation or double phase formation with a certain composition in ferrous materials. The single phase consists of Fe_2B layer whereas the double phase formation consists of FeB layer and Fe_2B layer. Double phase is formed when the boron medium is excessed. Extra boron atom will form a rich-phase FeB layer on the Fe_2B layer. This rich phase FeB layer is brittle than Fe_2B layer. The thickness of boride layer varies parabolic with time by referring to the equation 1 (Topuz *et* *al* ,.2015). The equation 2 shows the relationship between the growth rate constant, activation energy and temperature. The equation 2 is taking natural logarithm and converts to equation 3.

$$x = \sqrt{Kt} \tag{1}$$

where,

x is the thickness of boride layer (cm),

K is the growth rate constant (cm^2/s), and

t is the time of boronizing (s).

$$K = K_o \times \exp(-\frac{Q}{RT}) \tag{2}$$

$$In(K) = In(K_o) - (\frac{Q}{RT}) \tag{3}$$

where,

K is the growth rate constant (m^2/s),

Q is the activation energy (J/mol),

T is the temperature of boronizing (K).

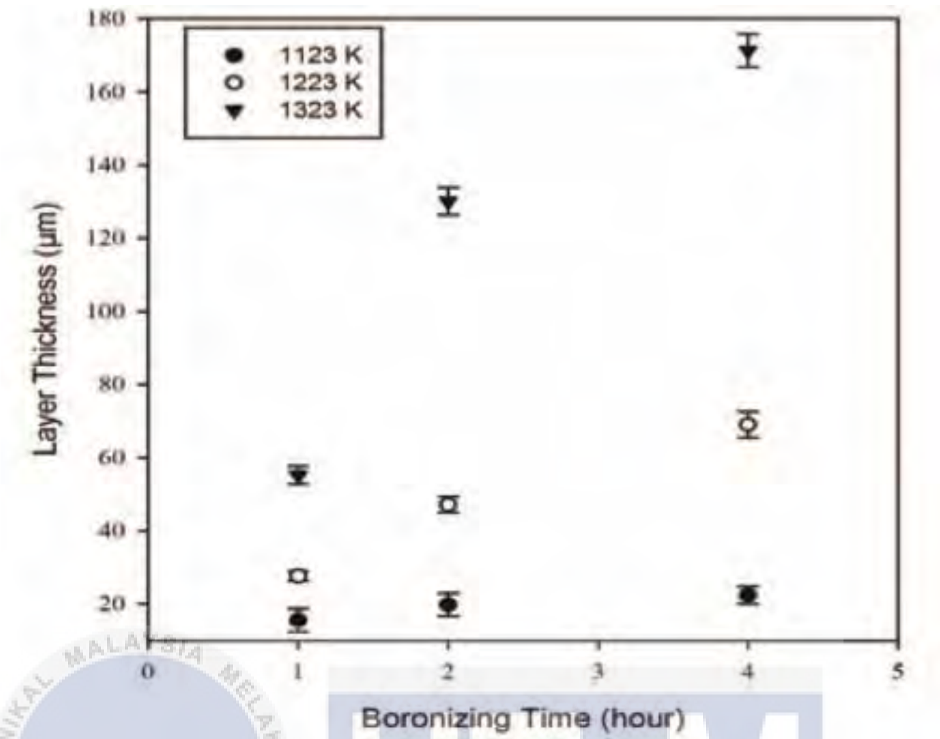

Figure 2.2: Thickness of boride layer is proportional to temperature and time (Topuz *et al*., 2015)

2.1.4 Application of boronizing

Boronizing is famous and wise choice in boronizing technologies due to its low and high technology. Boronizing has low operating cost and high quality which can increase the wear resistance, hardness, and reduce the coefficient of friction of metal. These effect makes boronizing become a fine choice in tooling application as shown in Table 2.2.

Table 2.2:Application of boronizing (Adapted from Suwattananont, 2004)

Substrate material			Application
AISI	BSI	DIN	
		St37	Bushes, bolts, nozzles, conveyer tubes, base plates, runner, blades, thread guides
1020	-	C15(Ck15)	Gear drives, pump shafts
1043	-	C45	Pins, guide rings, grinding disk, bolts
		St50-1	Casting inserts, nozzles, handles
1138	-	45S20	Shaft protection sleeves, mandrels
1042	-	Ck45	Swirl elements, nozzles (for oil bumpers), rollers, bolts, gate plates
		C45W3	Gate plates
W1	-	C60W3	Clamping chucks, guide bars
D3	-	X210Cr12	Bushes, press tools, plates, mandrels, punches, dies
C2	-	115CrV3	Drawing dies, ejectors, guides, insert pins
		40CrMnMo7	Gate plates, bending dies
H11	BH11	X38CrMoV51	Plungers, injection cylinders, spruce
H13	-	X40CrMoV51	Orifices, ingot molds, upper and lower dies and matrices for hot forming, disks
H10	-	X32CrMoV33	Injection molding dies, fillers, upper and lower dies and matrices for hot forming
D2	-	X155CrVMo121	Threaded rollers, shaping and pressing rollers, pressing dies and matrices
		105WCr6	Engraving rollers
D6	-	X210CrW12	Straightening rollers
S1	~BS1	60WCrV7	Press and drawing matrices, mandrels, liners, dies, necking rings
D2		X165CrVMo12	Drawing dies, rollers for cold mills
L6	BS224	56NiCrMoV7	Extrusion dies, bolts, casting inserts

		X45NiCrMo4	Embossing dies, pressure pad and dies
02	~BO2	90MnCrV8	Molds, bending dies, press tools, engraving rollers, bushes, drawing dies, guide bars, disks, piercing punches
E52100	-	100Cr6	Balls, rollers, guide bars, guides
		Ni36	Parts for nonferrous metal casting equipment
		X50CrMnNiV229	Parts for unmagnetizable tools (heat treatable)
4140	708A42 (En19C)	42CrMo4	Press tools and dies, extruder screws, rollers, extruder barrels, non-return valves
4150	~708A42 (CDS-15)	50CrMo4	Nozzles base plates
4317	-	17CrNiMo6	Bevel gears, screw and wheel gears, shafts, chain components
5115	-	16MnCr5	Helical gear wheels, guide bars, guiding columns
6152	-	50CrV4	Thrust plates, clamping devices, valve springs, spring contacts
302	302S25 (EN58A)	X12CrNi188	Screw cases, bushes
316	316S16 (EN58J)	X5CrNiMo1810	Perforated or slotted hole screens, parts for the textile and rubber industries
		G-X10CrNiMo189	Valve plugs, parts for the textile and chemical industries
410	410S21 (En56A)	X10Cr13	Valve components, fittings
420	~420S45 (EN56D)	X40Cr13	Valve components, plunger rods, fitting, guides, parts for chemical plants
		X35CrMo17	Shaft, spindles, valves
Gray and ductile cast iron			Parts for textile machinery, mandrels, molds

2.2 ADVANTAGES AND DISADVANTAGES OF BORONIZING

2.2.1 Advantages

The advantages of boronizing treatment are (Davis, 2002):

- Iron boride layers have exceedingly high hardness of strength value (1600HV – 2000HV) which is higher than other conventional surface hardening treatment.
- It has low surface coefficient of friction.
- Boride layer's hardness can be maintained at any temperature.
- Suitable for most of the steel category.
- Corrosion-erosion resistance of ferrous materials in non-oxidizing dilute acid can be enhanced.
- It has medium oxidation resistance (1550 F).
- Borided parts have longer lifespan.

2.2.2 Disadvantages

The disadvantages of boronizing treatment are (Davis, 2002):

- The process are inflexible and preferably labor intensive.
- Boronizing's growth is 5% to 25% of the boride layer thickness and it's hard to control.
- It is only diamond lapping can partially remove the boride layer. Thus, precise boronizing is usually practiced for part with huge cross-sectional area.

2.3 MILD STEEL

Mild steel is under ferrous metal category. Mild steel has good welding properties. It is acceptable for drilling, machining, heat treating and even forging. Chemical composition of mild steel is consist of 0.25%-0.29% carbon, 0.2% copper, 98% iron, 1.03% manganese, 0.04% phosphorous, 0.28% silicon and 0.05% sulfur (Azom, 2012). Mild steel is also called as low carbon steel. It is a low cost material and softer compare to medium carbon steel and high carbon steel. Mild steel hardness can be enhanced by boronizing at temperature between 899°C and 927°C. Table 2.3 shows the mechanical properties of mild steel.

Table 2.3: Mechanical properties of mild steel (Adapted from Azom, 2012)

Mechanical Properties	Metric	Imperial
Tensile Strength, Ultimate	400-550MPa	58000-79800 psi
Tensile Strength, Yield	250MPa	36300 psi
Modulus of Elasticity	200GPa	29000ksi
Bulk Modulus	140GPa	20300ksi
Poissons Ratio	0.260	0.260
Shear Modulus	79.3GPa	11500ksi

CHAPTER 3

DETAIL OF METHODOLOGY

3.1 Flow chart

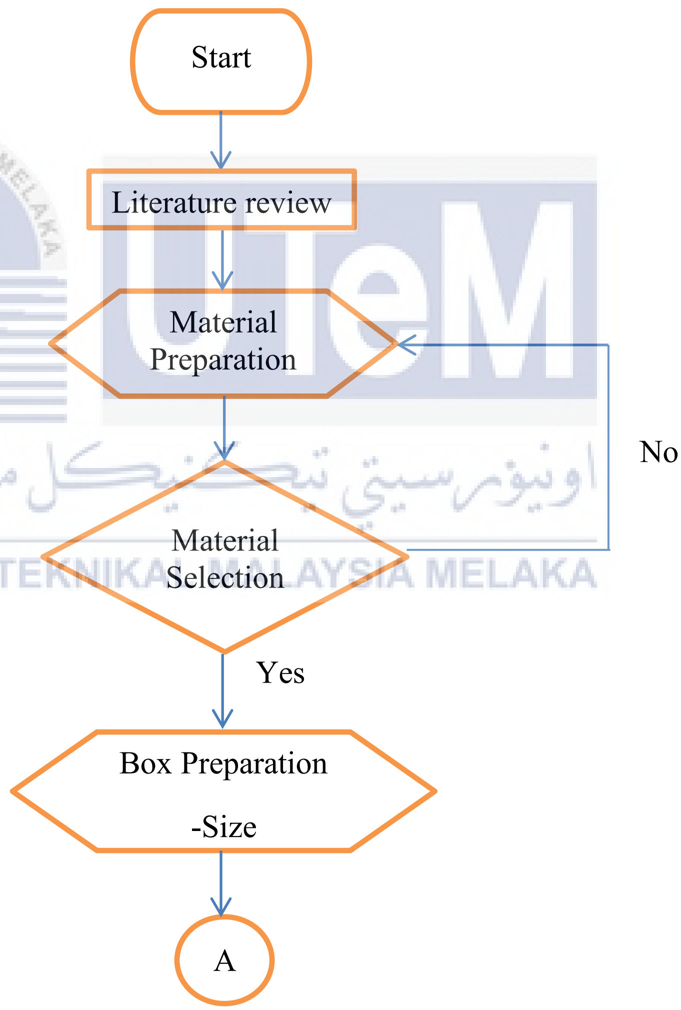

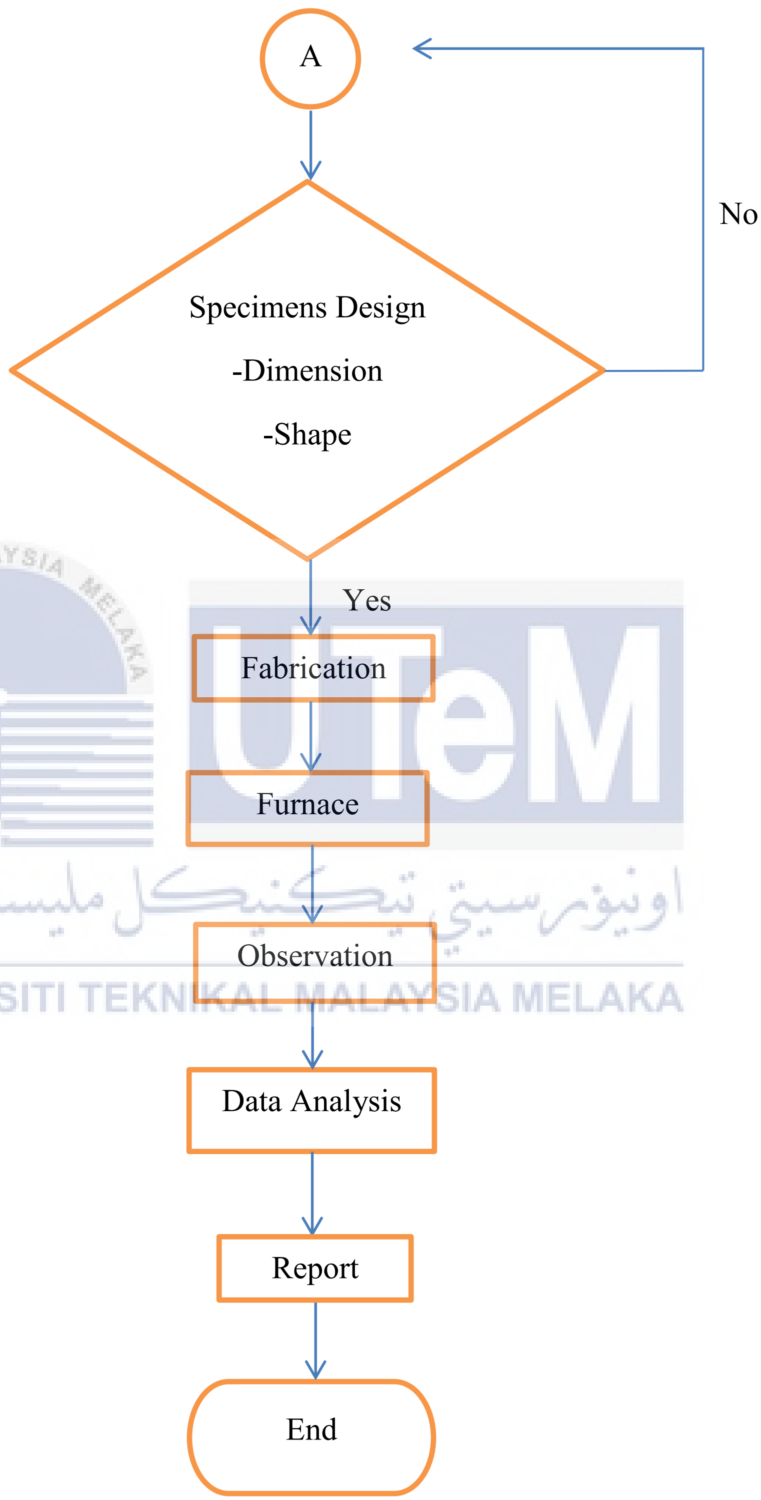
A
No
Specimens Design
-Dimension
-Shape
Yes
Fabrication
Furnace
Observation
Data Analysis
Report
End

3.2 GANTT CHART

PSM I

Activities	Week														
	01	02	03	04	05	06	07	08	09	10	11	12	13	14	15
Briefing and planning	■														
Literature review		■	■	■	■	■	■	■	■	■	■	■	■	■	■
Material preparation		■	■												
Fabrication				■	■	■	■	■							
Boronizing process									■	■	■	■	■		
Draft report		■	■	■	■	■	■	■	■						
PSM I final report		■	■	■	■	■	■	■	■	■	■	■	■	■	
Seminar I															■

PSM II

Activities	Week														
	01	02	03	04	05	06	07	08	09	10	11	12	13	14	15
Briefing and planning	■														
Literature review		■	■	■	■	■	■	■	■	■	■	■	■	■	■
Observation and result			■	■	■	■	■								
PSM II final report	■	■	■	■	■	■	■	■	■	■	■	■	■	■	■
Seminar II															■

3.3 DESIGNS OF SPECIMEN

The container' height that is provided in the laboratory is 40mm. These containers will be filled with 10mm height boronizing powder on top and at bottom of specimen. 20mm×20mm×20mm cube specimen is designed as shown in Figure 3.1. Four shapes are selected for the grooved geometry surfaces which are U-shaped (rectangular), 2mm C-shaped (circular), 4mm C-shaped (circular) and V-shaped (triangular) as shown in Figure 3.2. All grooves are allocated on the cube specimens and the isometric view is shown in Figure 3.3. The four design specimens are drawn by using Solid work software.

Figure 3.1 20mm×20mm×20mm cube specimen

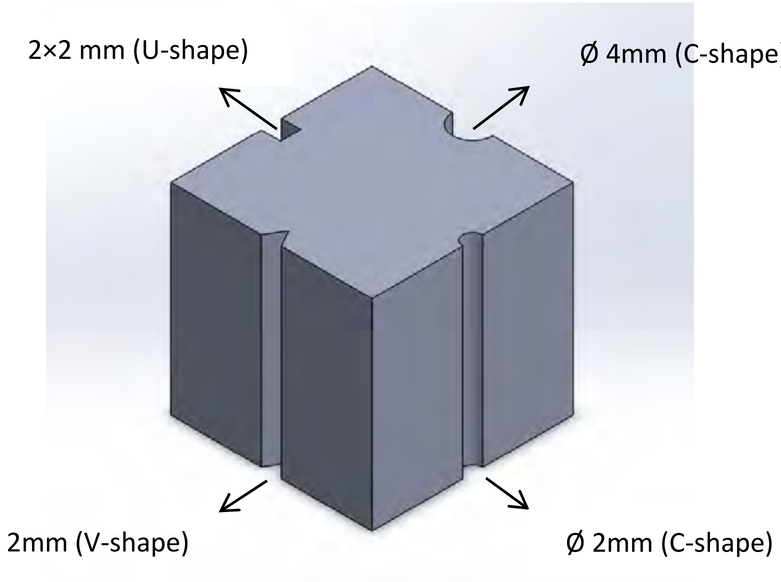

Figure 3.2 Design on specimen

Figure 3.3 Isometric view of four designs

3.4 PREPARATION OF SPECIMENS

The designs are prepared for fabrication. Nine specimens are needed in this project.

3.4.1 Material

The material used in this project is mild steel. Mild steel is a low carbon steel and its chemical composition consist of 0.25%-0.29% carbon, 0.2% copper, 98% iron, 1.03% manganese, 0.04% phosphorous, 0.28% silicon and 0.05% sulfur (Azom, 2012). Mild steel rod is provided in Faculty of Mechanical Engineering lab of Universiti Teknikal Malaysia Melaka as shown in Figure 3.4. It is a rectangular mild steel rod. The width and height of mild steel rod is 35mm × 35mm. The length of mild steel is 900mm.

Figure 3.4: Mild steel rectangular rod

3.4.2 Apparatus

Two apparatus are used in this project which is bandsaw cutting machine, computer numerical control machine (CNC) and polishing machine. Bandsaw cutting machine is a machine that cut steel accurately compared to other manual apparatus as shown in Figure 3.5. The mild steel rod is placed perpendicular to the bandsaw blade and the cutting length is 30mm per pieces. The power of machine is turned on. The speed of cutting is adjusted to cut the mild steel rod into 9 pieces of cube as shown in Figure 3.6. The mild steel cube dimension is 30mm×35mm×35mm.

Figure 3.5: Bandsaw cutting machine

Figure 3.6: Cutting process of mild steel rod

Computer numerical control milling machine is programed by using computer. The code, drawing and axis can be controlled by using the computer. The code and drawing can be saved in the computer memory as well. CNC milling machine has high accuracy, stable processing quality and high rigidity. The cutting and molding can carry out at multi coordinates, move along multiple axis and adaptable to all complex parts. Commonly CNC milling machines is used to perform cutting, drilling and molding of various materials.

In this project, CNC milling machine is used to mold the 30mm×35mm×35mm mild steel cube into 20mm×20mm×20mm mild steel cube. The axis of molding is adjusted by using the computer. There are three axes which is Y-axis, X-axis and Z-axis. The Y-axis, X-axis and Z-axis are set as -10mm, 40mm, and 0mm for top face of cube as shown in Figure 3.7. The top face of 30mm×35mm×35mm mild steel cube is placed at the base and fixed as shown in Figure 3.8. The door of machine is closed and the molding process is started.

The process is repeated on remaining five faces according to the dimension needed to obtain 20mm×20mm×20mm mild steel cube.

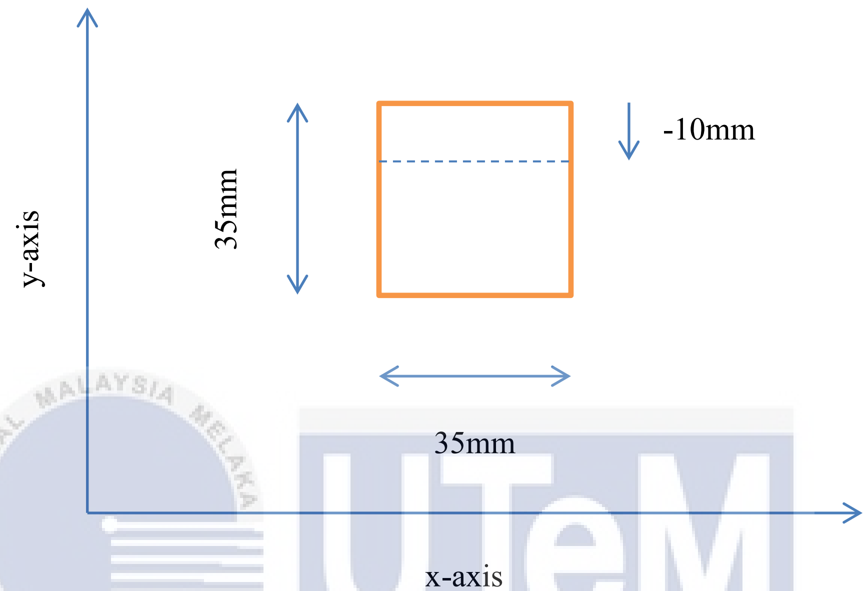

Figure 3.7: Y and X axis of 30mm×35mm×35mm mild steel cube

Figure 3.8: The mild steel is fixed at the base of machine

Nine pieces of 20mm×20mm×20mm mild steel cube is mounted as shown in Figure 3.9. The four designs are mounted on the nine pieces of 20mm×20mm ×20mm mild steel cube by using CNC milling machines as shown in Figure 3.10.

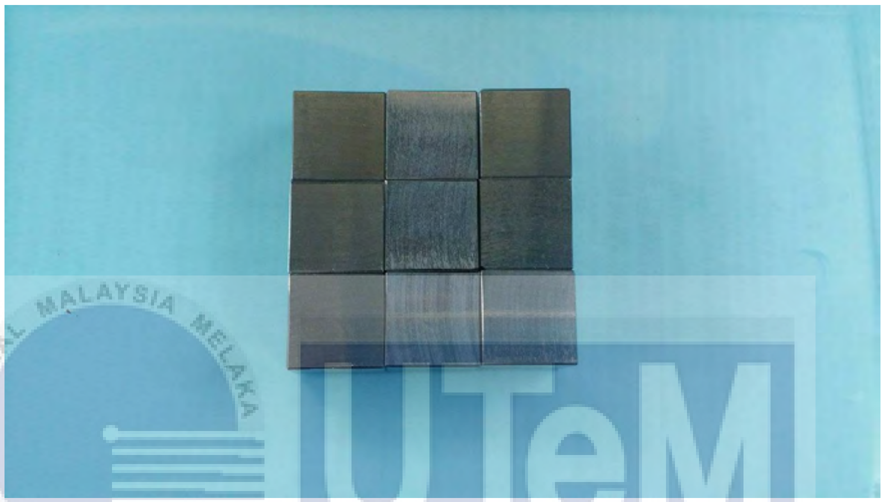

Figure 3.9: Nine pieces of 20mm×20mm×20mm mild steel cube

Figure 3.10: Four Designs are molded on the 20mm×20mm×20mm mild steel cube

The nine specimens is cleaned with acetone and placed into a plastic container. The silica gel is put into the plastic container to absorb moisture and prevent the mild steel cubes rust. The acetone and silica gel are shown in Figure 3.11.

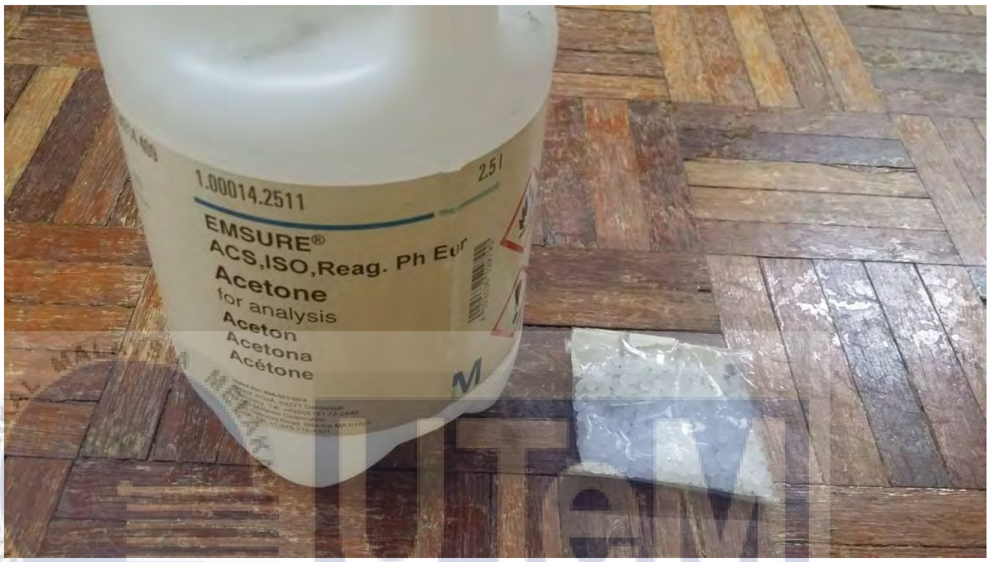

Figure 3.11: Acetone and silica gel

3.5 BORONIZING

3.5.1 Preparation

Six container is prepared and provided in Faculty of Mechanical Engineering lab of Universiti Teknikal Malaysia Melaka. The diameter of containers is 65mm as shown in Figure 3.12. It is acted as a container for the specimen to boronize.

The boronizing powder provided in Faculty of Mechanical Engineering lab of Universiti Teknikal Malaysia Melaka is Ekabor 1 as shown in Figure 3.13. Ekabor 1has small grain size which is 150μm and high density which is 1.9 g/cm^3.

Figure 3.12: Containers and lid

Figure 3.13: Boronizing powder (Ekabor 1)

3.5.2 Procedure

There are 6 steps of boronizing process:

1. The container is filled with 10mm boronizing powder as shown in Figure 3.14.

Figure 3.14: Container Filled with 10mm boronizing powder

2. The specimen is placed into the center of container (on the 10mm boronizing powder) as shown in Figure 3.15.

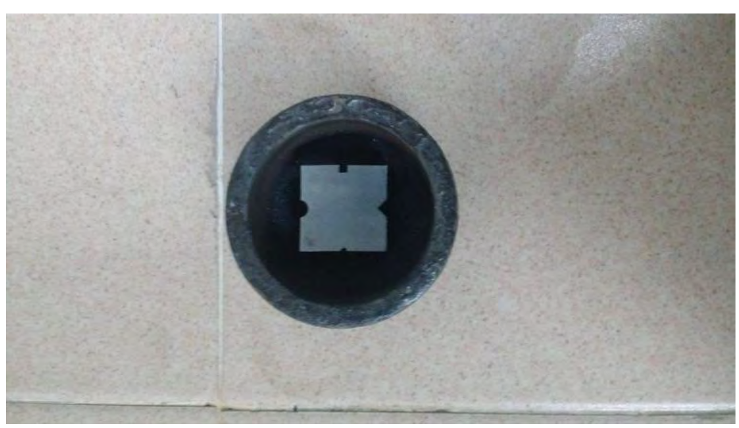

Figure 3.15: The specimen is placed into the container

3. The container is fully filled with boronizing powder and covered with lid as shown in Figure 3.16. The schematic diagram of container is shown in Figure 3.17.

Figure 3.16: The container is fully filled with boronizing powder and covered with lid

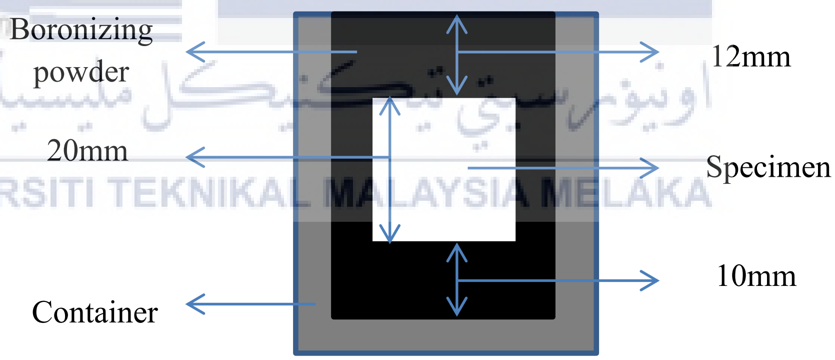

Figure 3.17: Schematic diagram of container

4. The containers are placed into the furnace for heating process. The heating temperature will be set as 850°C as shown in Figure 3.18.

Figure 3.18: Heating process inside furnace

5. The containers are removed from furnace after 2 hours, 4 hours and 6 hours. The containers are cooled down at room temperature as shown in Figure 3.19.

Figure 3.19: Containers cool down in room temperature

6. Step 1 to step 5 is repeated with 900°C and 950°C.

The boronizing schematic diagram is as shown in figure 3.20. The containers are cooled and proceed to characterization.

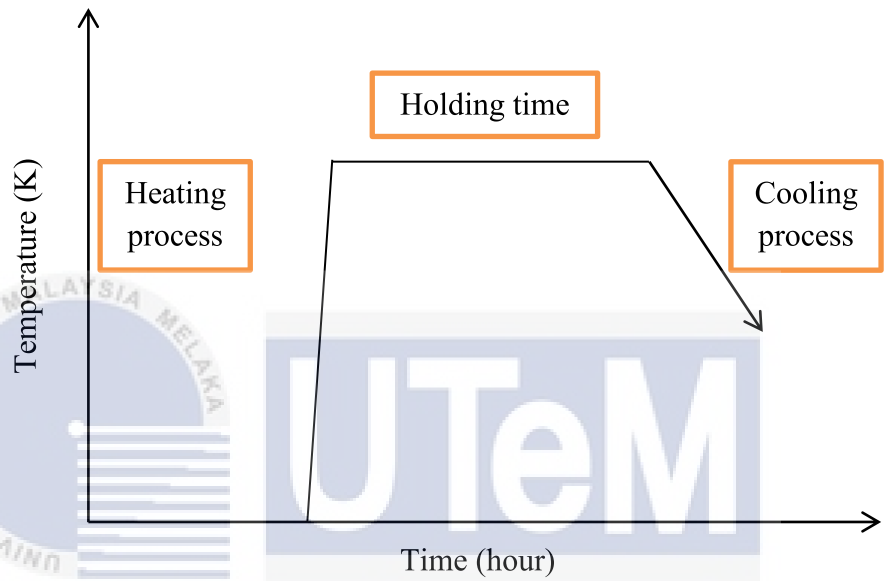

Figure 3.20: Schematic diagram for boronizing process

3.6 CHARACTERIZATION

The specimens are removed from the containers. The specimens are grinded on a rotating sand paper as shown in Figure 3.21. The water is poured during the grinding operation to lower the specimen's temperature. The specimens are polished on a rotating disc of abrasive paper after grinded as shown in Figure 3.22.

The specimens are undergone the etching process as shown in Figure 3.23. Etching is used to review the structural characteristics of mild steel. The specimens are then progressed to metallographic analysis. Metallography is the study of metals by optical microscopes.

Metallographic analysis can perceive macrostructures which cannot be observed by the naked eye or under low magnifications. Metallographic can analyse the grain size, corrosion analysis, boronizing thickness, and phase analysis. Optical microscopes will be used in metallographic analysis as shown in Figure 3.24.

Figure 3.21: Grinding the specimens

Figure 3.22: Polishing the specimens

Figure 3.23: Etching

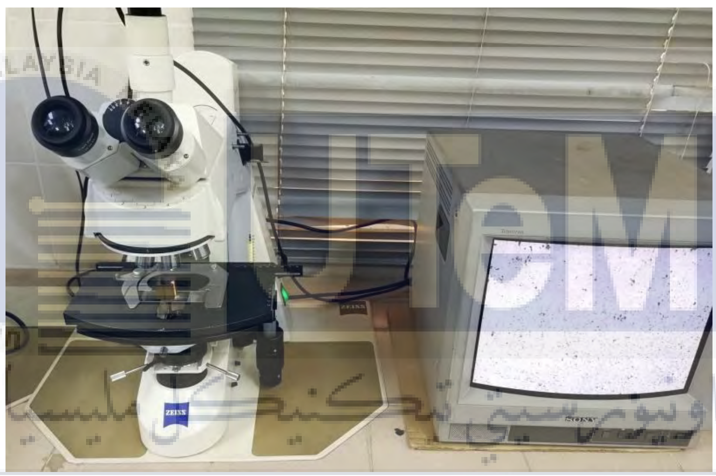

Figure 3.24: Metallographic analysis

CHAPTER 4

RESULT AND ANALYSIS

4.1 SEM CROSS SECTIONAL VIEW

There were 9 specimens in this project. Each of the specimens has four different grooved geometries designs which is U-shaped (rectangular), 2mm C-shaped (circular), 4mm C-shaped (circular) and V-shaped (triangular). These shapes have different boride layer thickness due to the different of boronizing time and temperature. The boronizing time is 2 hours, 4 hours and 6 hours respectively. The temperature is 1123K, 1173K and 1223K respectively.These shapes are observed by using Scanning Electron Microscopes and inverted microscope which is provided in Faculty of Mechanical Engineering lab of Universiti Teknikal Malaysia Melaka. Figure 4.1(a), (b), (c) and (d) show the SEM cross sectional view and boride layer of different grooved surface.

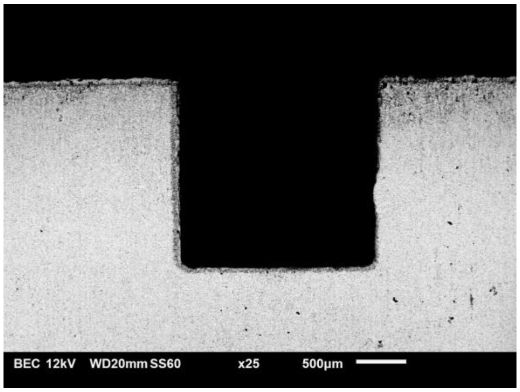

(a)

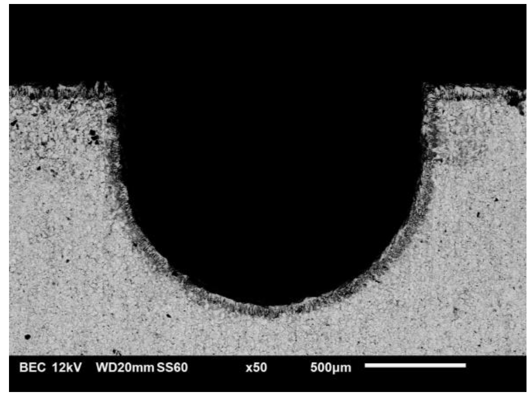

(b)

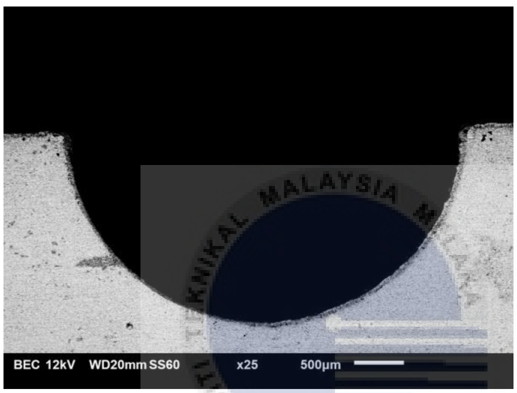

(c)

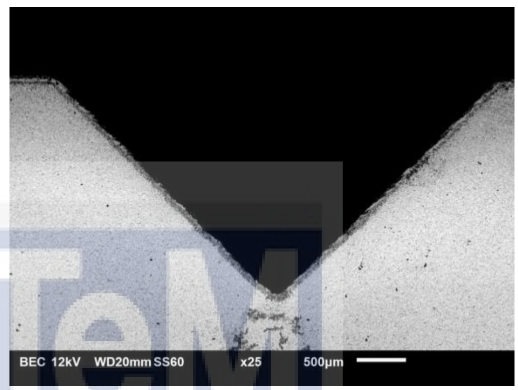

(d)

Figure 4.1: SEM image of (a) U-shaped, (b) 2mm C-shaped, (c) 4mm C-shaped, (d) V-shaped

(after boronizing at 1123K for 4 hours)

4.2 BORONIZING OF U-SHAPED (RECTANGULAR)

4.2.1 Boride layer thickness

Figure 4.2 shows the boride layer of U-shaped. The thickness of boride layer on U-shaped is measured and recorded in Table 4.1. The boride layer thickness ranged from 31.347µm to 153.197µm depend on the boronizing time and temperature. Figure 4.3 shows parabolic plot based on the boride later thickness of U-shaped at different temperature and time.

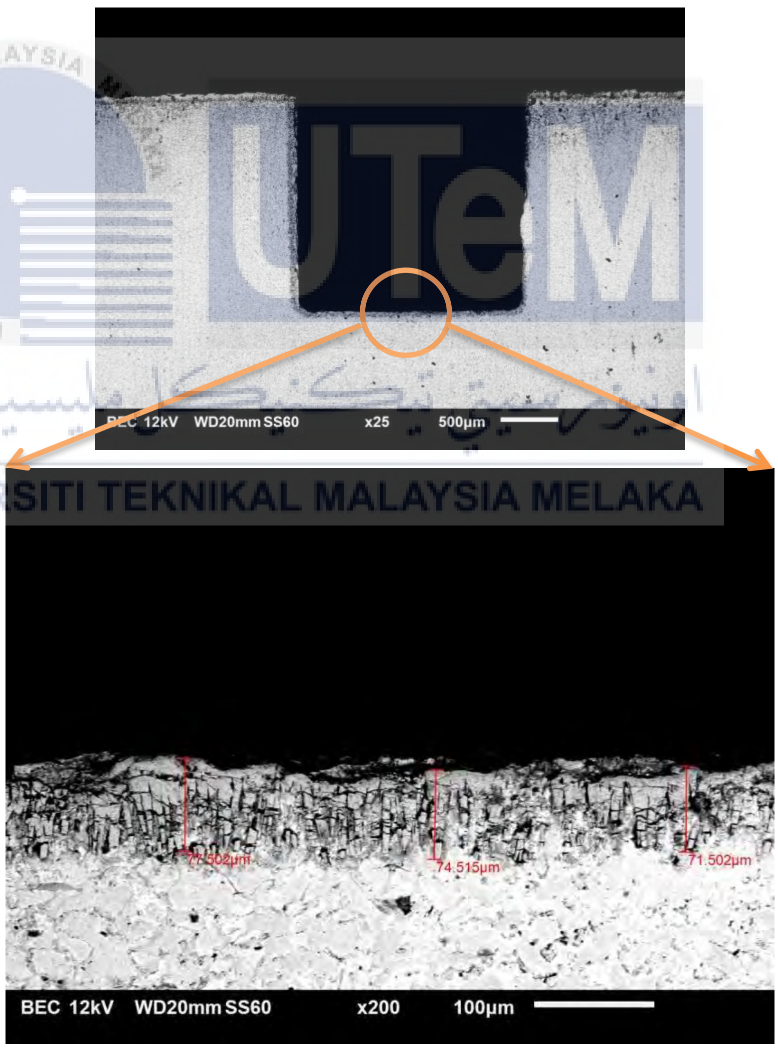

Figure 4.2: SEM cross sectional view of U-shaped at 1123K for 4 hours

Table 4.1: Boride layer thickness of U-shaped at different time and temperature

Temperature (K)	Time (hour)	Boride layer thickness (µm)			
		Point 1	Point 2	Point 3	Average (±Standard deviation)
1123	2	32.003	33.034	29.004	31.347 ± 2.0936
	4	77.502	74.515	71.502	74.506 ± 3.0000
	6	70.029	67.030	71.544	69.534 ± 2.2973
1173	2	40.112	39.579	42.450	40.714 ± 1.5271
	4	54.502	60.002	53.537	56.014 ± 3.4875
	6	99.511	121.501	115.553	111.755 ± 11.3746
1223	2	104.860	88.729	112.928	102.047 ± 12.3214
	4	101.640	133.370	149.150	128.053 ± 24.1971
	6	142.560	158.570	158.460	153.197 ± 9.2118

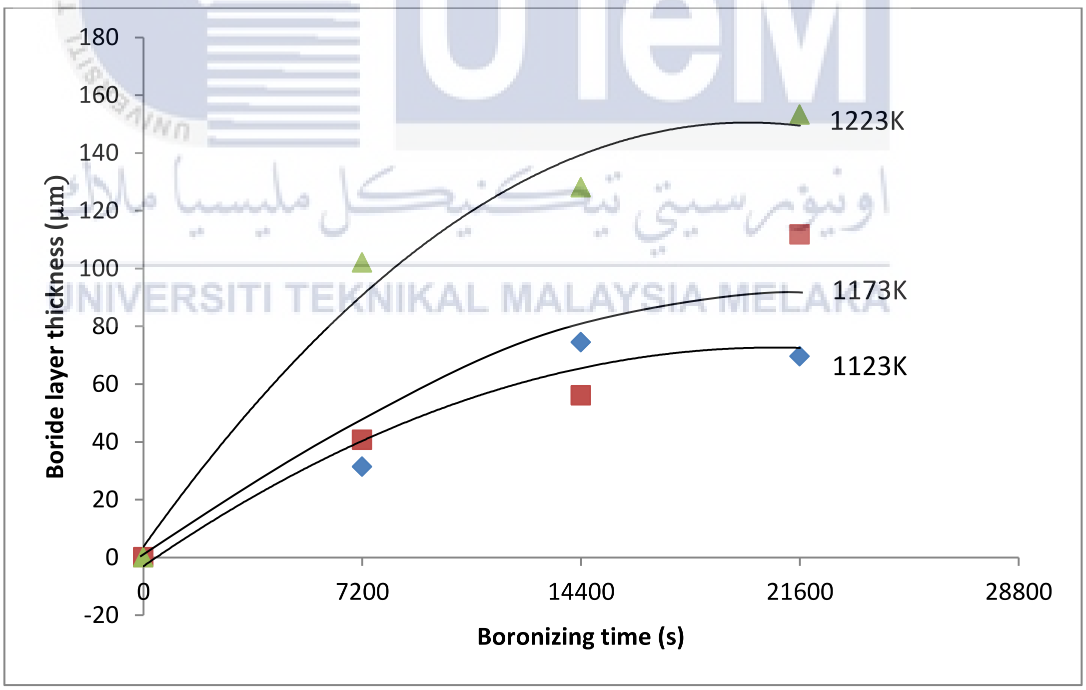

Figure 4.3: The variation of boride layer thickness against boronizing time for U-shaped

4.2.2 Activation Energy Analysis

The thickness of boride layer varies parabolic with time by referring to the equation 1 (Topuz *et al* ,.2015). Thus, the activation energy can be calculated by using equation 1. The graph of square of boride layer thickness against boronizing time for U-shaped is plotted as shown in Figure 4.4. The graph shows the square of boride layer changes linearly with time for U-shaped. The values of boron growth rate can be obtained from the gradient of the graph.

$$x = \sqrt{Kt} \tag{1}$$

where x is the thickness of boride layer (μm), K is the growth rate constant (m^2/s), and t is the time of boronizing (s).

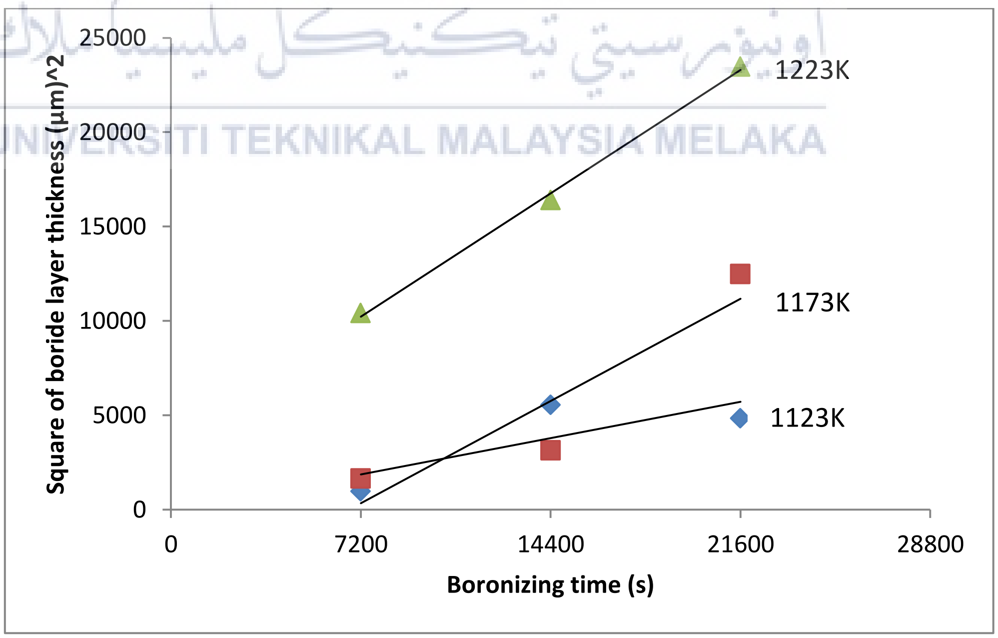

Figure 4.4: Square of boride layer thickness against boronizing time for U-shaped

The equation 2 shows the relationship between the growth rate constant, activation energy and temperature. The equation 2 is taking natural logarithm and converts to equation 3.

$$K = K_o \times \exp(-\frac{Q}{RT}) \qquad (2)$$

$$In(K) = In(K_o) - (\frac{Q}{RT}) \qquad (3)$$

where, K is the growth rate constant (m^2/s), Q is the activation energy (J/mol), K_0 is the pre exponential constant and R is the gas constant which is 8.314 $Jmol^{-1}K^{-1}$. In K (m^2s^{-1}) against $T^{-1}(K^{-1})$ for U-shaped is plotted as shown in Figure 4.5. The K values are ranged from 2.675× 10^{-13} m^2s^{-1} to 9.066×$10^{-13}m^2s^{-1}$. The activation energy of U-shaped is calculated as 148.64 $kJmol^{-1}$ and pre-exponential constant, K_0 is 2×$10^{-6}m^2s^{-1}$.

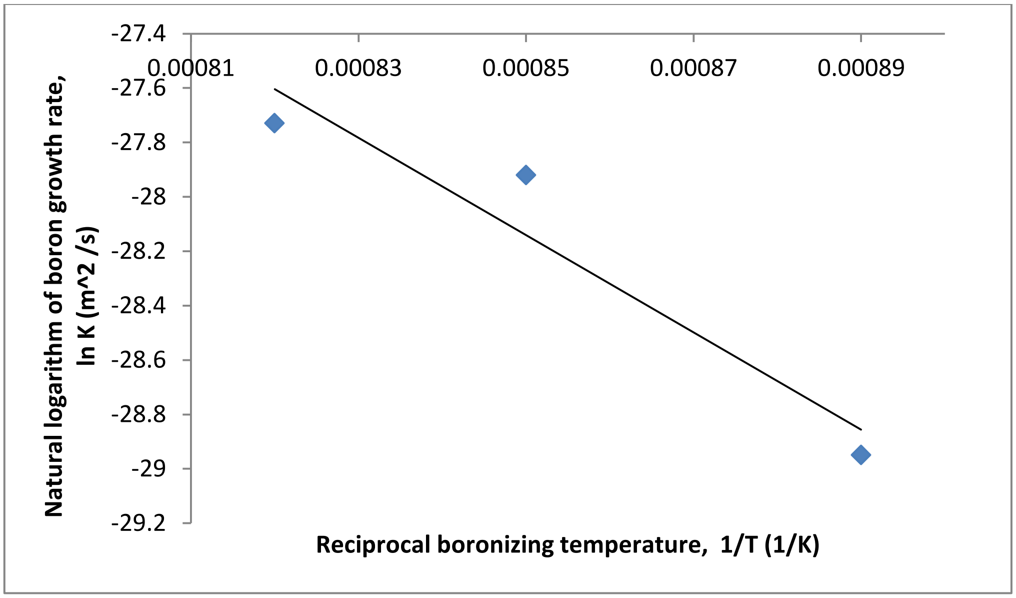

Figure 4.5: Natural logarithm of boron growth rate against reciprocal boronizing temperature for U-shaped

4.3 BORONIZING OF 2MM C-SHAPED (CIRCULAR)

4.3.1 Boride layer thickness

Figure 4.6 shows the boride layer of 2mm C-shaped. The thickness of boride layer on 2mm C-shaped is measured and recorded in Table 4.2. The boride layer thickness ranged from 35.689µm to 170.677µm depends on the boronizing time and temperature. Figure 4.7 shows parabolic plot based on the boride later thickness of 2mm C-shaped at different temperature and time.

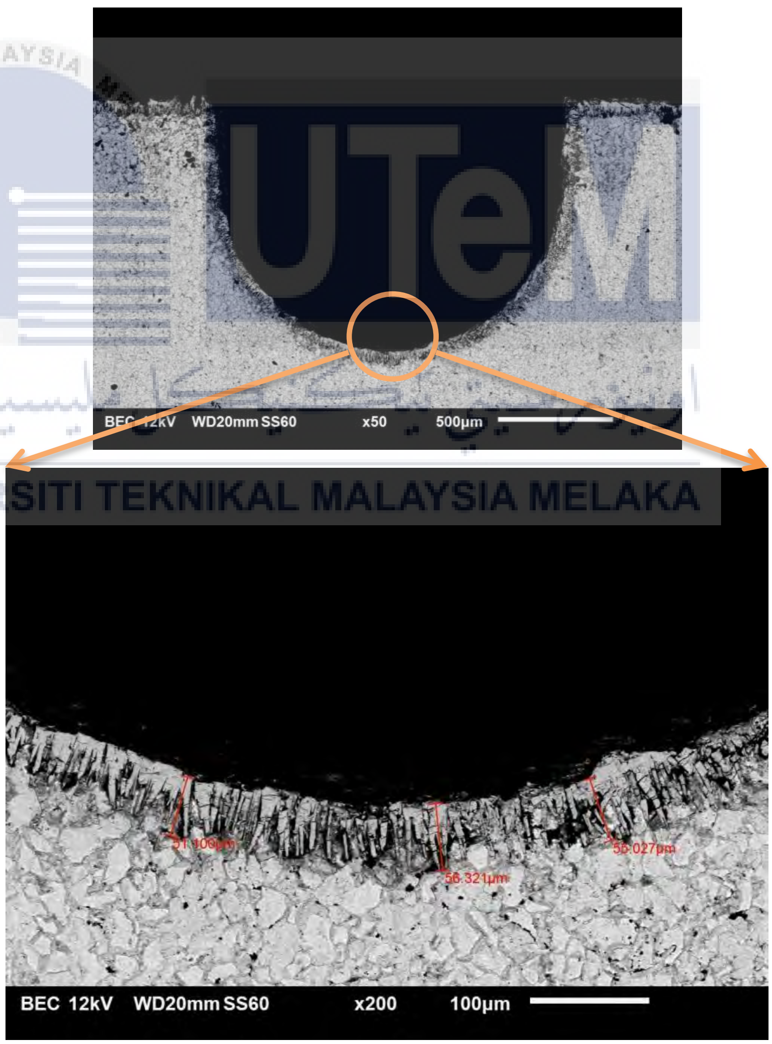

Figure 4.6: SEM cross sectional view of 2mm C-shaped at 1123K for 2 hours

Table 4.2: Boride layer thickness of 2mm C-shaped at different time and temperature

Temperature (K)	Time (hour)	Boride layer thickness (µm)			
		Point 1	Point 2	Point 3	Average (±Standard deviation)
1123	2	35.032	34.004	38.030	35.689 ± 2.0918
	4	51.100	56.321	55.027	54.149 ± 2.7189
	6	62.769	62.032	60.836	61.879 ± 0.9755
1173	2	73.934	84.006	69.378	75.773 ± 7.4853
	4	68.029	65.622	60.467	64.706 ± 3.8633
	6	118.950	116.039	117.478	117.489 ± 1.4555
1223	2	84.190	95.050	105.130	94.790 ± 10.4724
	4	153.590	133.110	124.520	137.073 ± 14.9348
	6	164.860	183.800	163.370	170.677 ± 11.3895

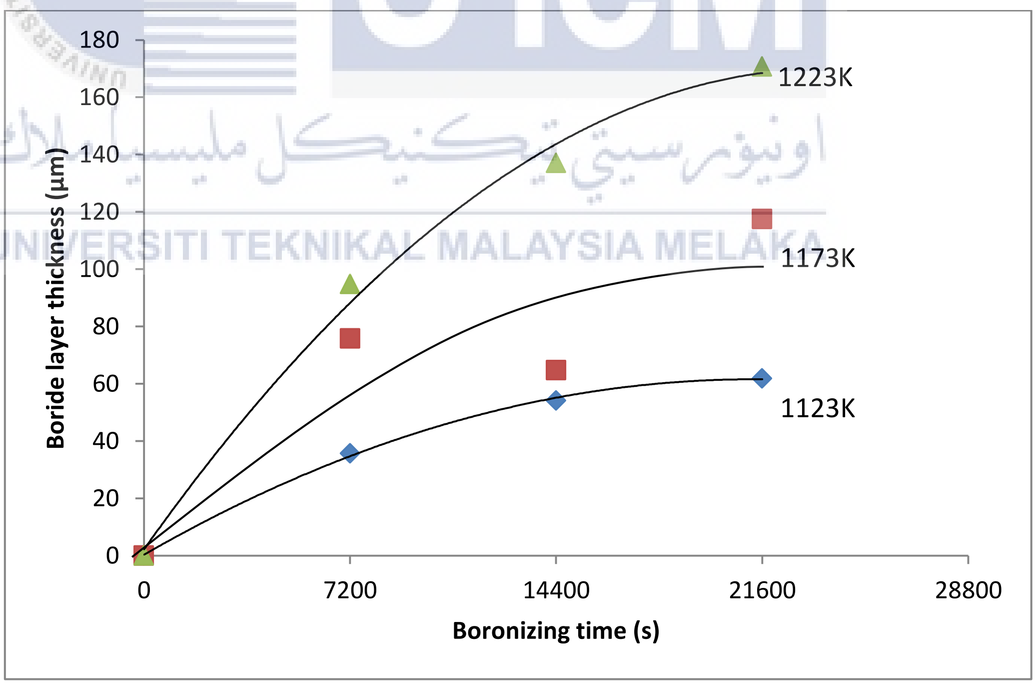

Figure 4.7: The variation of boride layer thickness against boronizing time for 2mm C-shaped

4.3.2 Activation Energy Analysis

The same analytical procedure as in subsection 4.2.2 is repeated. The graph of square of boride layer thickness against boronizing time for 2mm C-shaped is plotted as shown in Figure 4.8. ln K (m^2s^{-1}) against $T^{-1}(K^{-1})$ for 2mm C-shaped is plotted as shown in Figure 4.9. The K values are ranged from 1.774×10^{-13} m^2s^{-1} to 1.399×$10^{-12}m^2s^{-1}$. The activation energy of 2mm C-shaped is calculated as 244.36 $kJmol^{-1}$ and pre-exponential constant, K_0 is 4.124×$10^{-2}m^2s^{-1}$.

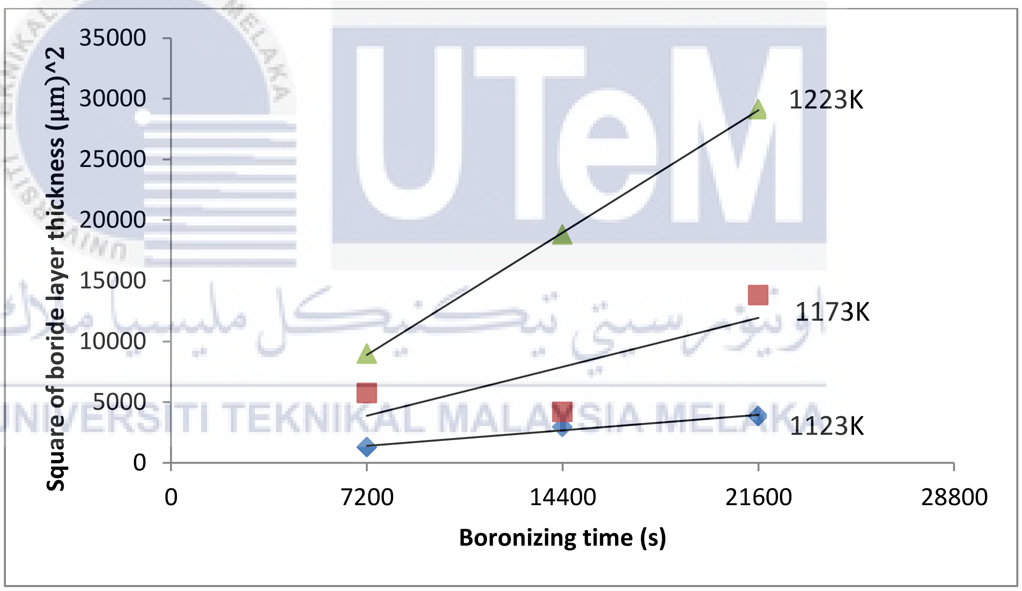

Figure 4.8: Square of boride layer thickness against boronizing time for 2mm C-shaped

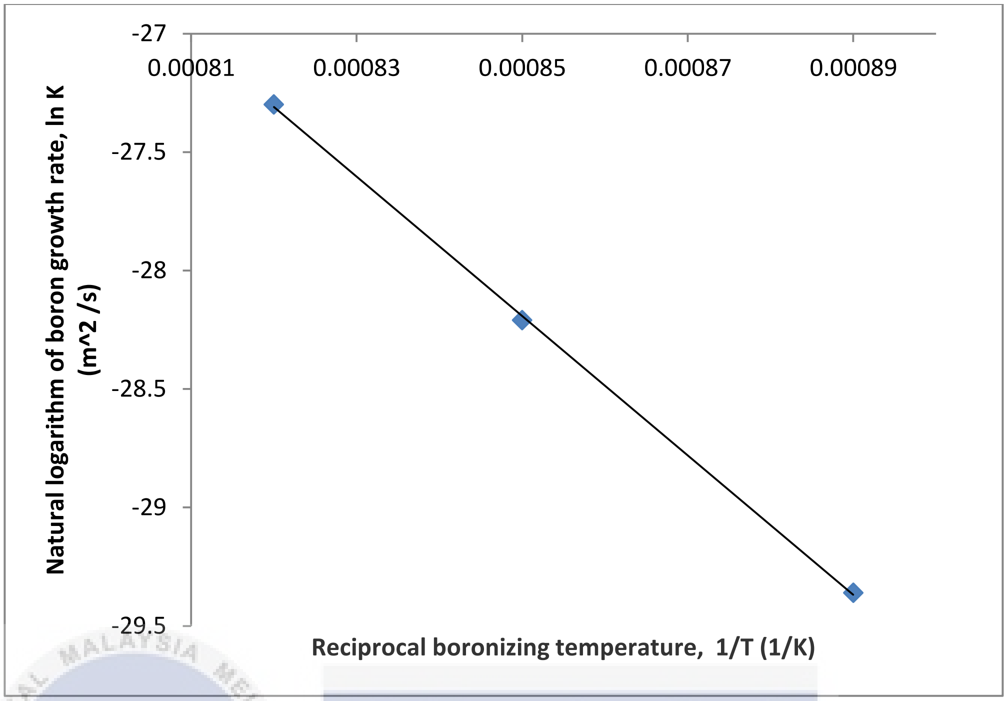

Figure 4.9: Natural logarithm of boron growth rate against reciprocal boronizing temperature for 2mm C-shaped

4.4 BORONIZING OF 4MM C-SHAPED (CIRCULAR)

4.4.1 Boride layer thickness

Figure 4.10 shows the boride layer of 4mm C-shaped. The thickness of boride layer on 4mm C-shaped is measured and recorded in Table 4.3. The boride layer thickness ranged from 29.575µm to 147.543µm depends on the boronizing time and temperature. Figure 4.11 shows parabolic plot based on the boride later thickness of 4mm C-shaped at different temperature and time.

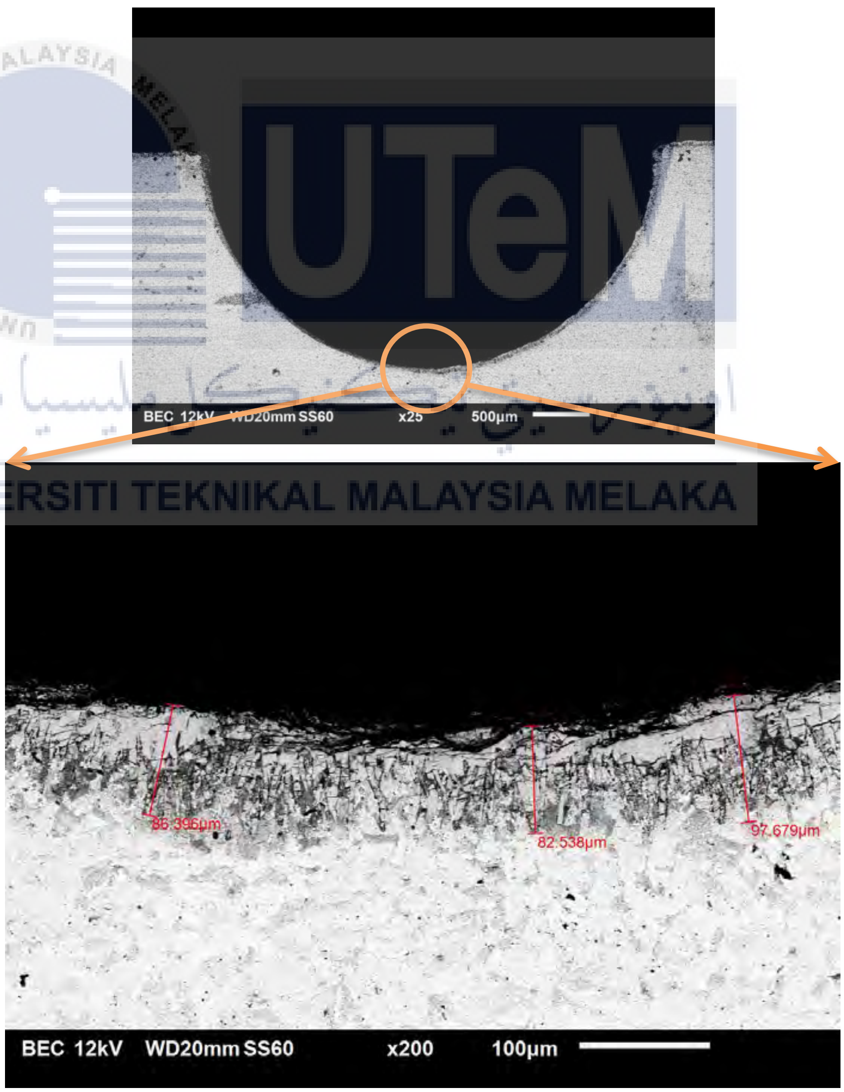

Figure 4.10: SEM cross sectional view of 4mm C-shaped at 1123K for 6 hours

Table 4.3: Boride layer thickness of 4mm C-shaped at different time and temperature

Temperature (K)	Time (hour)	Boride layer thickness (µm)			
		Point 1	Point 2	Point 3	Average (±Standard deviation)
1123	2	28.412	33.738	26.575	29.575 ± 3.7204
	4	45.003	51.039	44.026	46.689 ± 3.7984
	6	86.396	82.538	97.679	88.871 ± 7.8681
1173	2	38.965	42.240	46.198	42.468 ± 3.6219
	4	56.036	66.030	52.038	58.035 ± 7.2069
	6	110.010	110.018	113.748	111.259 ± 2.1558
1223	2	98.890	94.790	82.200	91.96 ± 8.6975
	4	211.740	168.660	182.420	187.607 ± 22.0034
	6	147.560	151.940	143.130	147.543 ± 4.4050

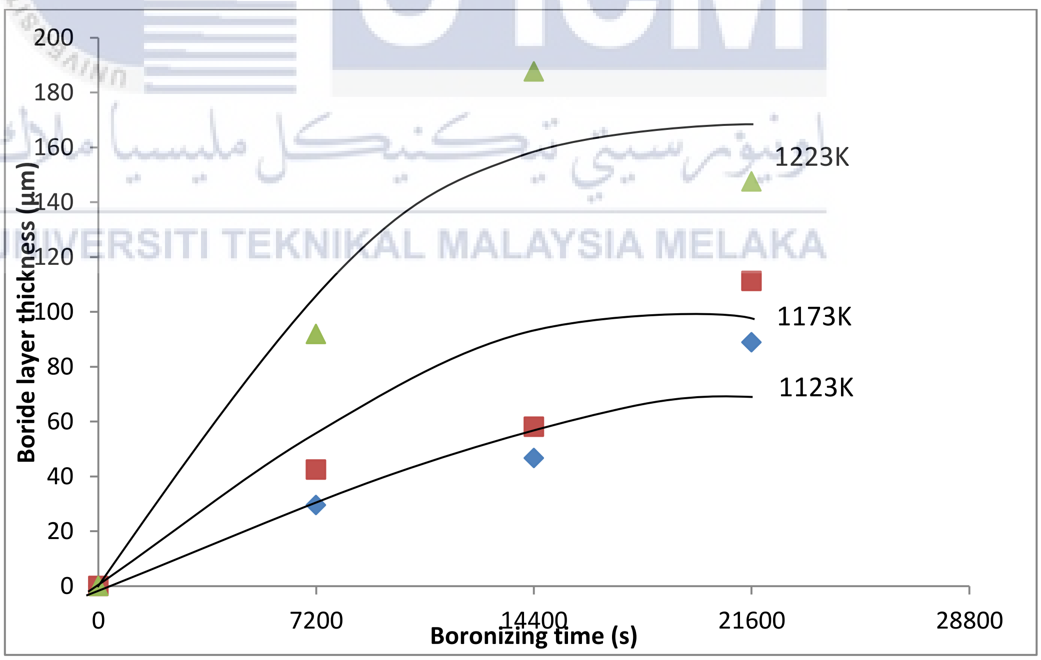

Figure 4.11: The variation of boride layer thickness against boronizing time for 4mm C-shaped

4.4.2 Activation Energy Analysis

The same analytical procedure as in subsection 4.2.2 is repeated. The graph of square of boride layer thickness against boronizing time for 4mm C-shaped is plotted as shown in Figure 4.12. ln K (m^2s^{-1}) against $T^{-1}(K^{-1})$ for 4mm C-shaped is plotted as shown in Figure 4.13. The K values are ranged from 4.877×10^{-13} m^2s^{-1} to 9.244×$10^{-13}m^2s^{-1}$. The activation energy of 4mm C-shaped is calculated as 76.51 $kJmol^{-1}$ and pre-exponential constant, K_0 is 1.77×$10^{-9}m^2s^{-1}$.

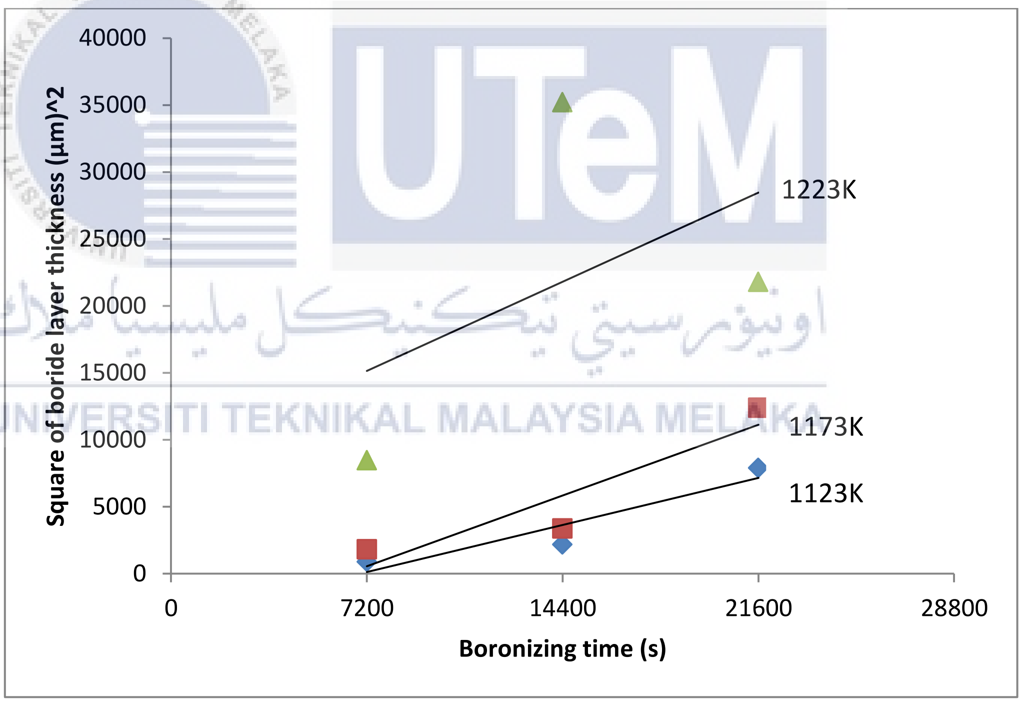

Figure 4.12: Square of boride layer thickness against boronizing time for 4mm C-shaped

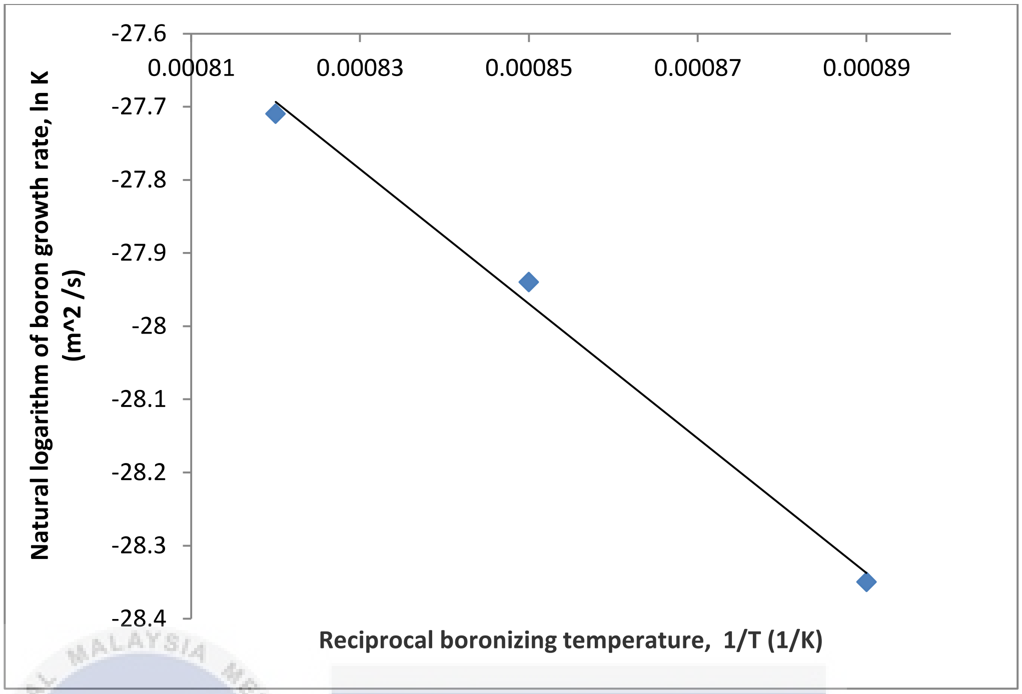

Figure 4.13: Natural logarithm of boron growth rate against reciprocal boronizing temperature for 4mm C-shaped

4.5 BORONIZING OF V-SHAPED

4.5.1 Boride layer thickness

Figure 4.14 shows the boride layer of V-shaped. The thickness of boride layer on V-shaped is measured and recorded in Table 4.4. The boride layer thickness ranged from 49.750µm to 186.41µm depends on the boronizing time and temperature. Figure 4.15 shows parabolic plot based on the boride later thickness of V-shaped at different temperature and time.

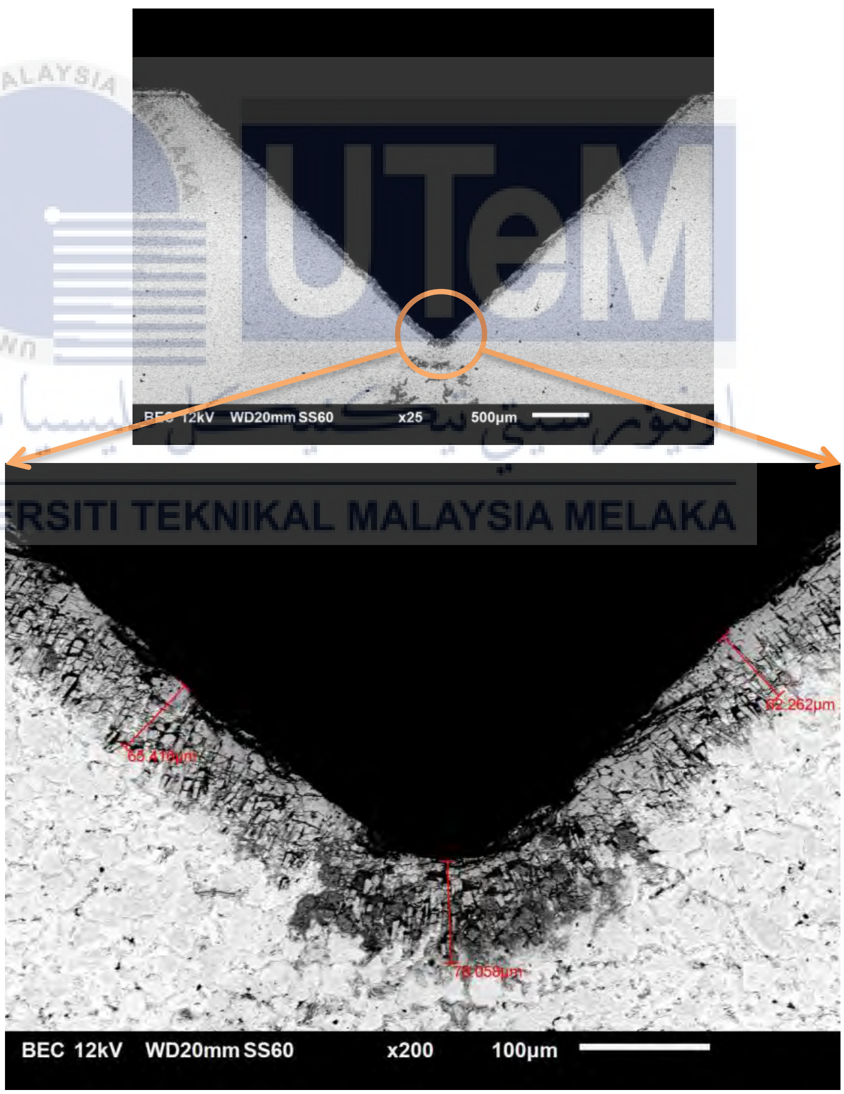

Figure 4.14: SEM cross sectional view of V-shaped at 1123K for 4 hours

Table 4.4: Boride layer thickness of V-shaped at different time and temperature

Temperature (K)	Time (hour)	Boride layer thickness (µm)			
		Point 1	Point 2	Point 3	Average (±Standard deviation)
1123	2	48.200	52.010	49.041	49.750 ± 2.0016
	4	62.262	73.058	65.410	66.910 ± 5.5521
	6	56.502	68.017	60.000	61.506 ± 5.9034
1173	2	54.000	54.148	44.000	50.716 ± 5.8167
	4	106.181	113.508	123.009	114.232 ± 8.4373
	6	85.550	95.901	101.843	94.431 ± 8.2453
1223	2	150.020	157.080	168.560	158.553 ± 9.3574
	4	138.040	131.940	138.140	136.040 ± 3.5511
	6	215.520	179.530	164.180	186.41 ± 26.3524

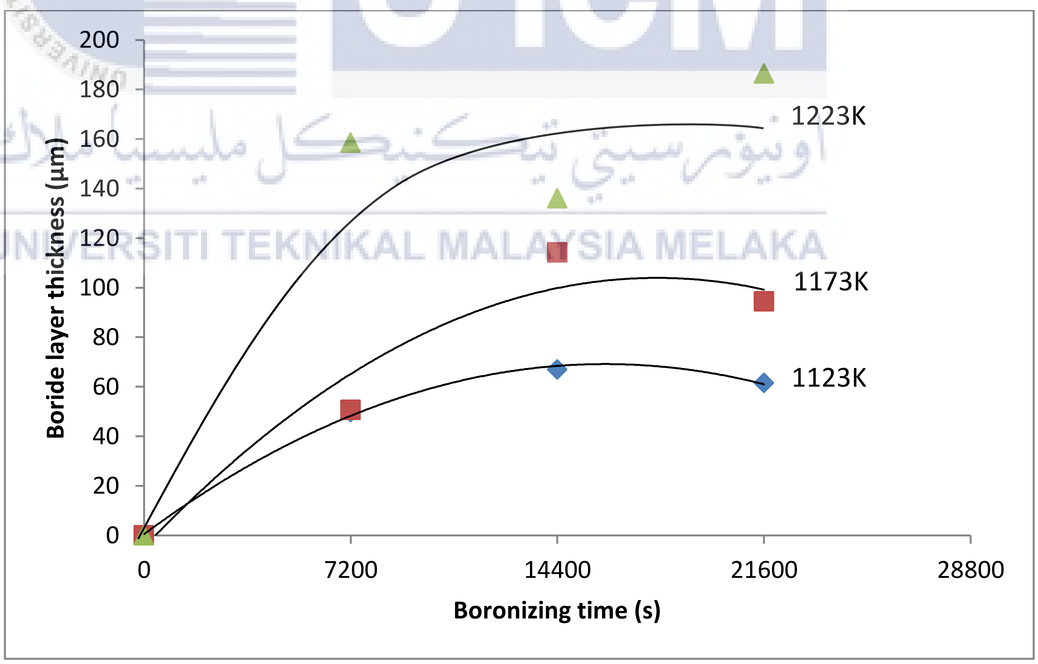

Figure 4.15: The variation of boride layer thickness against boronizing time for V-shaped

4.4.2 Activation Energy Analysis

The same analytical procedure as in subsection 4.2.2 is repeated. The graph of square of boride layer thickness against boronizing time for V-shaped is plotted as shown in Figure 4.16. ln K (m^2s^{-1}) against $T^{-1}(K^{-1})$ for V-shaped is plotted as shown in Figure 4.17. The K values are ranged from 9.082×10^{-14} m^2s^{-1} to 6.673×$10^{-13}m^2s^{-1}$. The activation energy of V-shaped is calculated as 241.33 $kJmol^{-1}$ and pre-exponential constant, K_0 is 1.526×$10^{-2}m^2s^{-1}$.

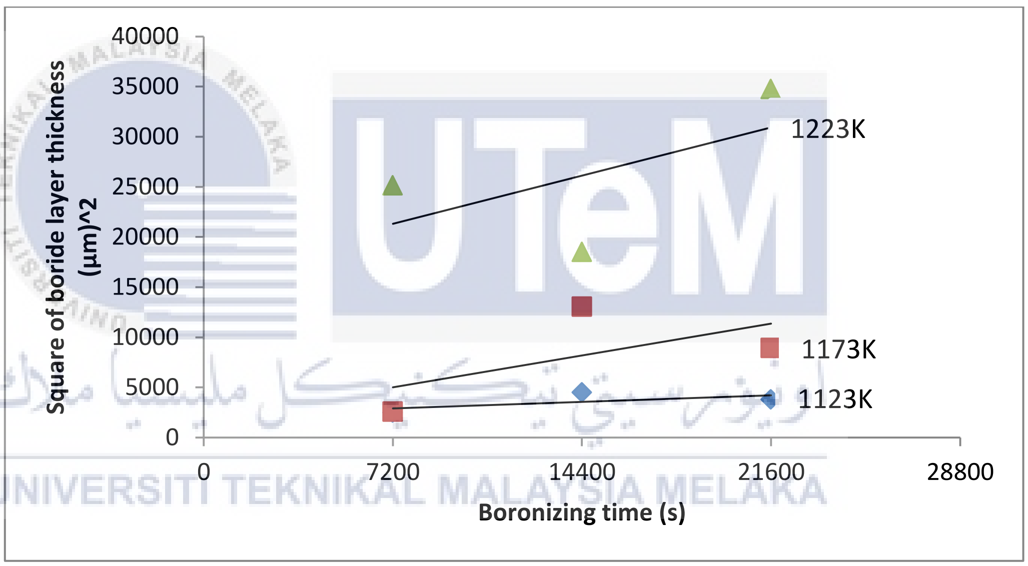

Figure 4.16: Square of boride layer thickness against boronizing time for V-shaped

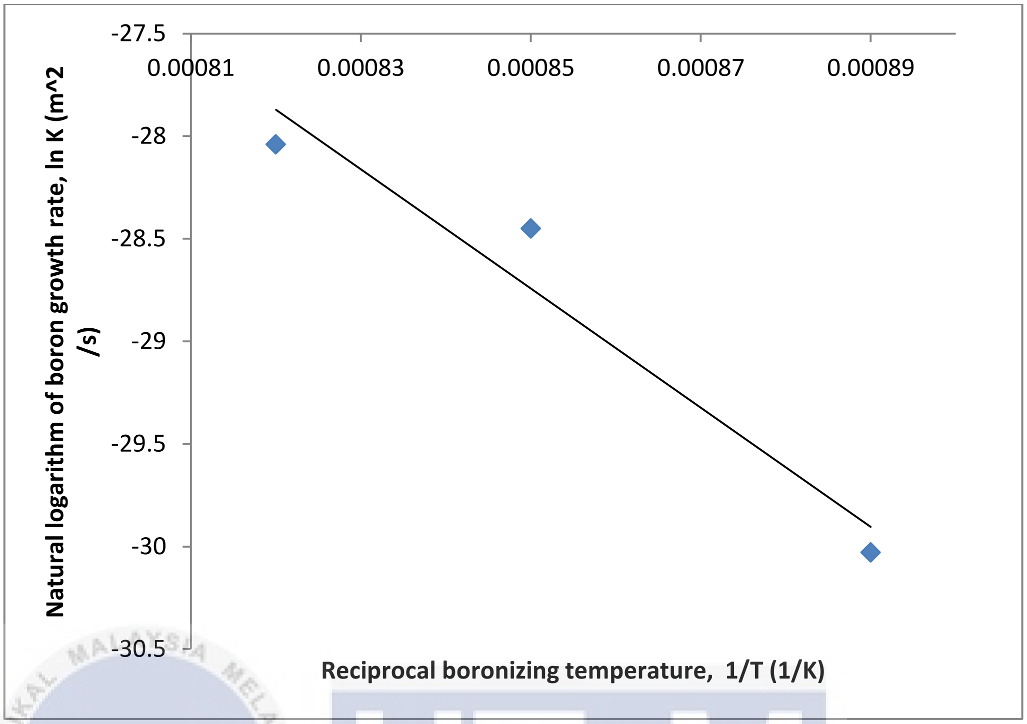

Figure 4.17: Natural logarithm of boron growth rate against reciprocal boronizing temperature for V-shaped

CHAPTER 5

DISCUSSION

5.1 CROSS SECTIONAL VIEW OF SPECIMENS

The specimen's material used in this project was mild steel. Mild steel is also called as low carbon steel. Thus, the specimen's boride layer thickness will be demonstrated in saw-tooth structure (Yu *et al*., 2002). Figure 5.1 proved that the specimen used in this project is low carbon steel and its boride layer thickness is saw-tooth structure.

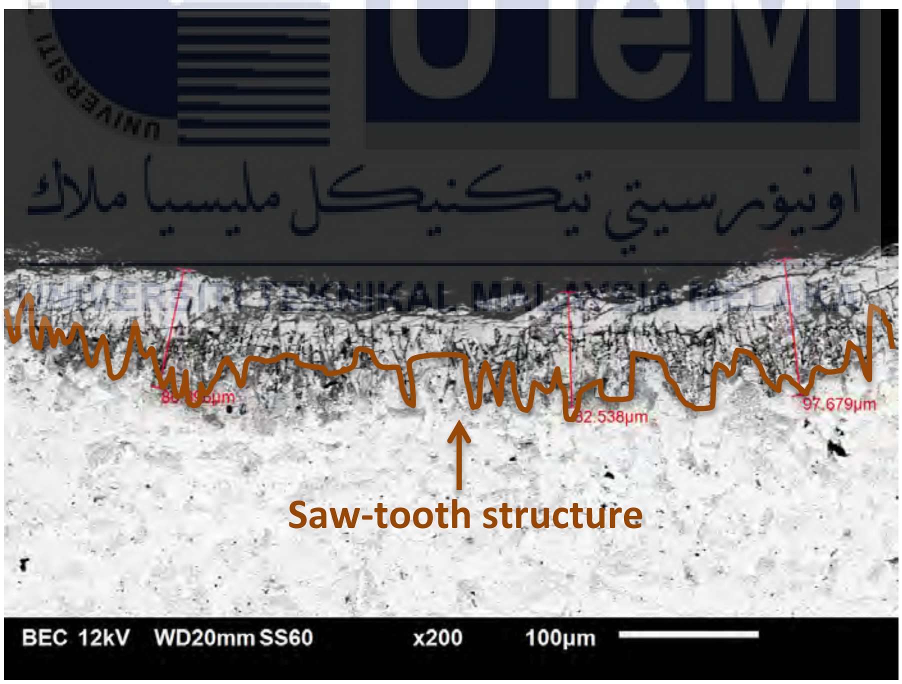

Figure 5.1: Boride thickness of mild steel (saw-tooth structure)

Mild steel is ferrous metals. Boron compound layer is formed on the specimen surface after boronizing process. The boron compound layer can be in single phase or double phase (Yorulmaz, 2007). In this project, the boron compound layer formed on the specimen's surface is single phase formation as shown in Figure 5.2. Single phase formation is consist of either $FeB\ or\ Fe_2B$.

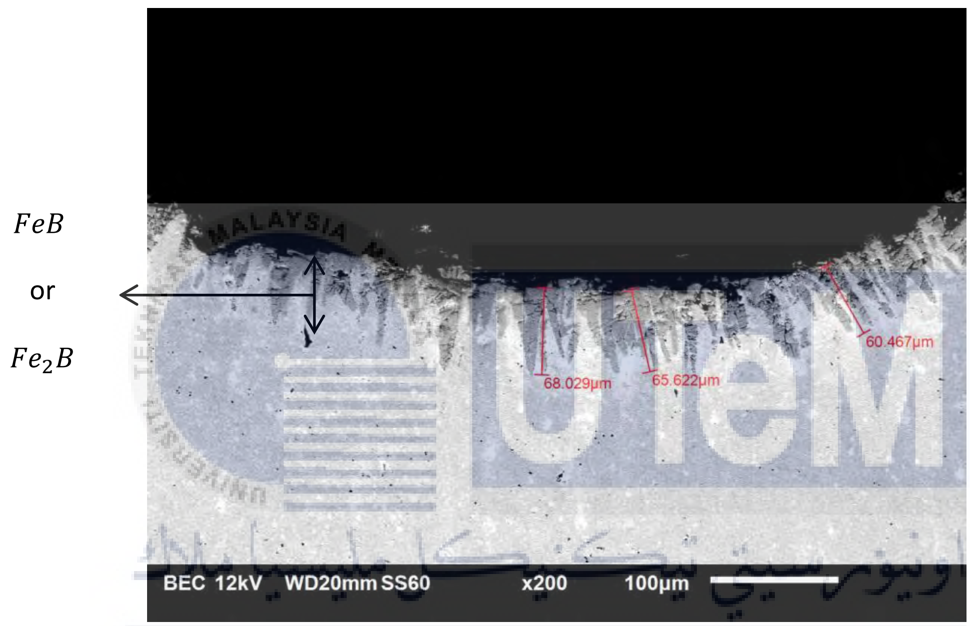

Figure 5.2: Single phase formation

5.2 BORIDE LAYER THICKNESS

Table 5.1 shows the boride layer thickness on different grooved surfaces. These different grooved surfaces consisted of four shapes which is U-shaped, 2mm C-shaped, 4mm C-shaped and V-shaped. Different shapes have different boride layer thickness depend on the boronizing time and temperature. U-shaped boride layer thickness ranged from 31.347 µm to 153.197 µm. 2mm C-shaped is ranged from 35.689 µm to 170.677 µm. 4mm C-shaped is ranged from 29.575 µm to 147.543 µm whereas V-shaped is ranged from 49.750 µm to 186.41 µm.

Table 5.1: Boride layer thickness on different grooved surfaces

Temperature (K)	Time (hour)	Boride layer thickness (µm) ± Standard Deviation			
		U-shaped	2mm C-shaped	4mm C-shaped	V-shaped
1123	2	31.347 ± 2.0936	35.689 ± 2.0918	29.575 ± 3.7204	49.750 ± 2.0016
	4	74.506 ± 3.0000	54.149 ± 2.7189	46.689 ± 3.7984	66.910 ± 5.5521
	6	69.534 ± 2.2973	61.879 ± 0.9755	88.871 ± 7.8681	61.506 ± 5.9034
1173	2	40.714 ± 1.5271	75.773 ± 7.4853	42.468 ± 3.6219	50.716 ± 5.8167
	4	56.014 ± 3.4875	64.706 ± 3.8633	58.035 ± 7.2069	114.232 ± 8.4373
	6	111.755 ± 11.3746	117.489 ± 1.4555	111.259 ± 2.1558	94.431 ± 8.2453
1223	2	102.047 ± 12.3214	94.790 ± 10.4724	91.96 ± 8.6975	158.553 ± 9.3574
	4	128.053 ± 24.1971	137.073 ± 14.9348	187.607 ± 22.0034	136.040 ± 3.5511
	6	153.197 ± 9.2118	170.677 ± 11.3895	147.543 ± 4.4050	186.41 ± 26.3524

Figure 5.3 shows the comparison of boride layer thickness on different grooved surfaces for 2 hours. The boride layer thickness on four grooved surfaces becomes thicker as the boronizing temperature increases. V-shaped has the highest thickness at 1123K and

1223K among the grooved surfaces for 2 hours specimen. The other three grooved shapes thickness are almost the same.

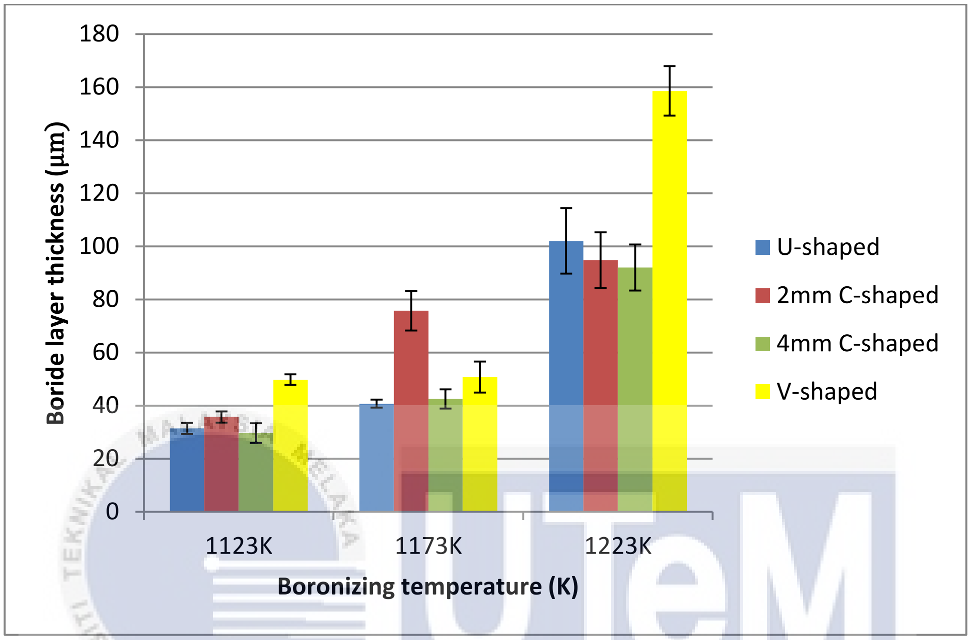

Figure 5.3: Boride layer thickness on different grooved surfaces for 2 hours

Figure 5.4 shows the comparison of boride layer thickness on different grooved surfaces for 4 hours. U-shaped has the highest thickness at 1123K. At 1173K, V-shaped has the highest thickness compare to other shapes. 4mm C-shaped has the highest thickness at 1223K whereas the other shapes thicknesses are almost the same.

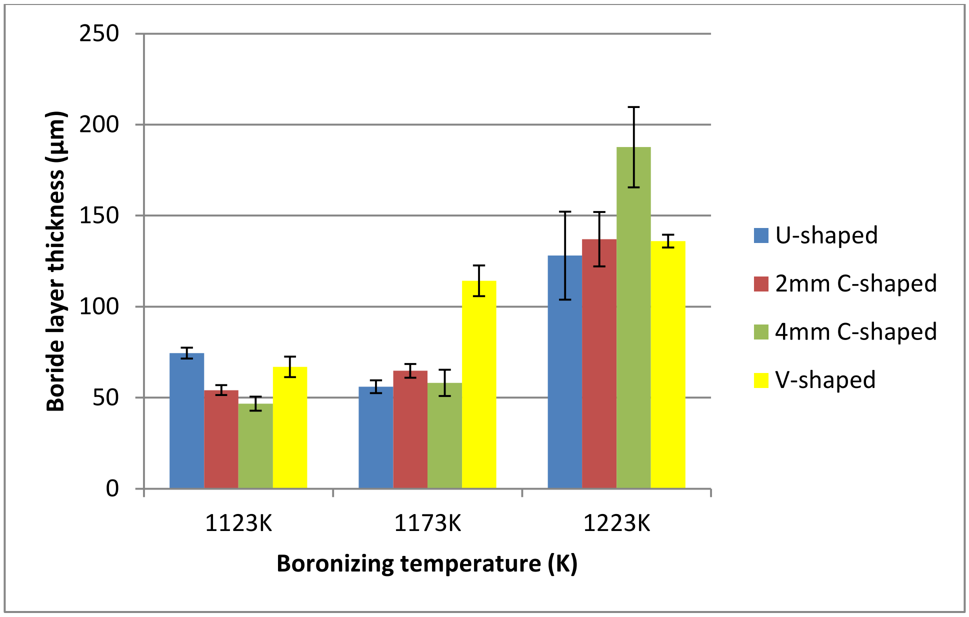

Figure 5.4: Boride layer thickness on different grooved surfaces for 4 hours

Figure 5.5 shows the comparison of boride layer thickness on different grooved surfaces for 6 hours. 4mm C-shaped has the highest thickness at 1123K for 6 hours and the other shapes thicknesses is almost the same. V-shaped has the highest thickness at 1223K. The consistency of the four grooved surfaces is almost the same.

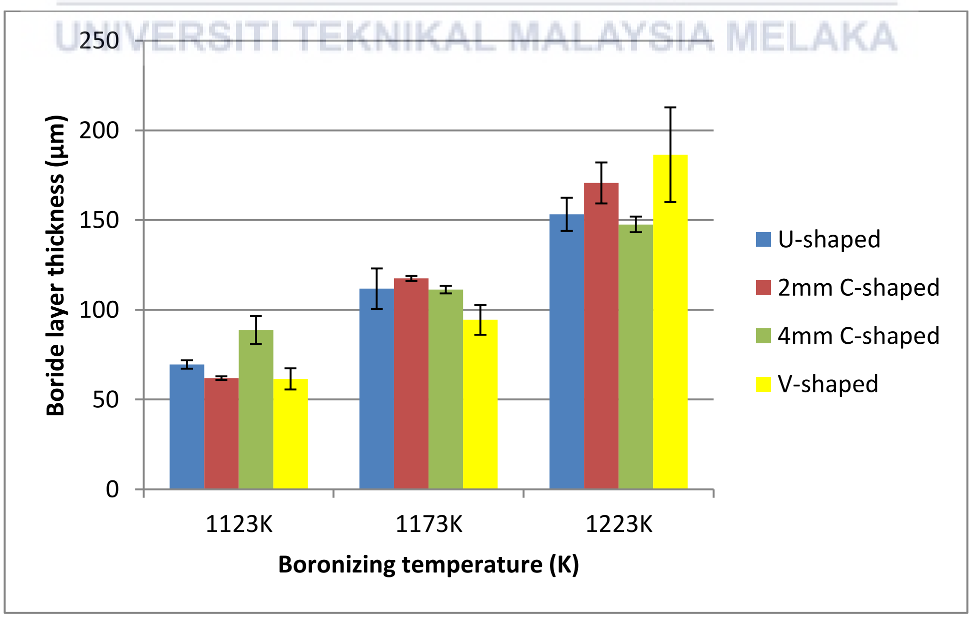

Figure 5.5: Boride layer thickness on different grooved surfaces for 6 hours

5.3 ACTIVATION ENERGY

Table 5.2 shows activation energy on different grooved surfaces. The activation energy for boronizing process of U-shape and 2mm C-shaped is 148.64 $kJmol^{-1}$ and 244.36 $kJmol^{-1}$ whereas the activation energy for boronizing process of 4mm C-shaped and V-shaped is 76.51 $kJmol^{-1}$ and 241.33$kJmol^{-1}$. 2mm C-shaped and V-shaped have the highest activation energy. The comparison of activation energy on different grooved surface is shown in Figure 5.6.

Table 5.2: Activation energy on different grooved surfaces

Grooved surface	Activation energy, Q
U-shaped	148.64 $kJmol^{-1}$
2mm C-shaped	244.36 $kJmol^{-1}$
4mm C-shaped	76.51 $kJmol^{-1}$
V-shaped	241.33 $kJmol^{-1}$

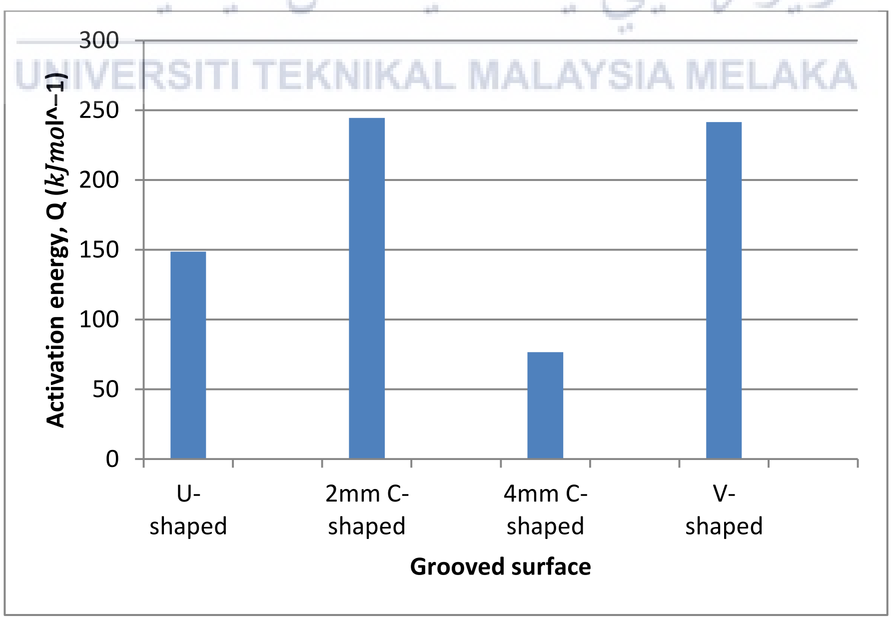

Figure 5.6: Comparison of activation energy on different grooved surface

Calik *et al*, 2008 stated that the geometry has no effect on the boride layer thickness. But according to this study, the result shows that the geometry does has effect on the boride layer thickness. The boride layer thickness values of geometries are different in this study. Beside, the activation energy of grooved geometries is different in this study. This situation proved that geometries does have effect on boride layer thickness. Unfortunately, the boride layer thickness of geometries are inconsistent. It might due to the sturcture of the furnace and the compaction of boron powder. The furnace used in this study is Narbertherm furnace. This furnace heater is designed at the side of the heating chamber. The specimen placed into the chamber will be heated from the side and resulting the side of the specimen will be boronized faster than other faces of the specimen.

CHAPTER 6

CONCLUSION AND RECOMMENDATION

6.1 CONCLUSION

The nine mild steel specimens were successfully boronized with different boronizing time and temperature. The boride layer thickness on different grooved surface were observed. The conclusions obtained from this study were as followed:

1. The temperature and time affected the boronizing thickness on grooved surfaces. The boride layer thickness increased as the temperature and time increased. U-shaped boride layer thickness ranged from 31.347 µm to 153.197 µm. 2mm C-shaped is ranged from 35.689 µm to 170.677 µm. 4mm C-shaped is ranged from 29.575 µm to 147.543 µm whereas V-shaped is ranged from 49.750 µm to 186.41 µm. The boride layer of specimens (low carbon steel) was demonstrated in saw-tooth structure.
2. The activation energy for boronizing on different grooved surface was different. 2mm-C-shaped has the highest activation energy which is 244.36 $kJmol^{-1}$ and 4mm C-shaped has the lowest activation energy which is 76.51 $kJmol^{-1}$.

6.2 RECOMMENDATION

The recommendation of this study is listed below:

1. Chamfer must be avoided at the edge of the specimen.
2. Extra set of specimen should be prepared to obtain accurate data.
3. Further study on ultimate stress and elongation on different geometries to differentiate the effect of boronizing on different geometries evidently.
4. Vertical furnace is recommended to carry out heating process.

REFERENCES

Arun ,S., Sivakuma ,T., Viswanathan ,P. & Subramanian ,R. (2013). Study of Hardness and Wear Properties of Boronized Aisi 4340 Steel. *International Journal of Engineering Research and Application*, 1927-1928.

Azom. (2012, July 5). *Azomaterial*. Retrieved December 3, 2016, from ASTM A36 Mild/Low Carbon Steel: http://www.azom.com/article.aspx?ArticleID=6117

Black, J.T., & Kohser, R.A. (2008). *DeGarmo's Materials and Processes in Manufacturing.* United States: Fowley, D.

Buijnsters, J.G., Shankar, P., & Gopalakrishnan, P. (2003). Diffusion-modified boride interlayers for chemical vapour deposition of low-residual-stress diamond films on steel substrates. *Thin Solid Films 426*, 85.

Calik, A. S. (2008). SpecimenGeometry Effect on the Mechanical Properties of AISI1040 Steel . *Naturforsch*, 448–452.

Davis, J. (2002). *Surface Hardening and Steels.* America: ASM Internasional.

Fichtl, W. (1981). Boronizing and its Practical Applications. *Materials in Engineering, Vol 2*, 278-279.

Jurci, P., & Hudakova, M. (2010). Microstructure of Boronized PM Cr-V Cold Work Ledeburitic Tool Steel. *Materials Engineering, Vol.17*, 20.

Kapoor, S. (2012). *High-Temperature Hardness and Wear Resistance of Stellite Alloys.* Canada: Patrimoine de I'edition.

Keddam , M., Dominguez ,M.O., Vargas ,O.A, Flores ,A., Renteria ,M.A., Esoinosa ,M., Barrientos ,A. (2015). Kinetic Study and Characterization of Borided AISI 4140 Steel. *Materials and Technologies*, 665-672.

Koorapati, E.P., Mohandas, K.N., Ramesh C.S. & Balashanmugan, N. (2013). Optimization of Surface Roughness during Hard Machining of Hard Chrome Plated Surfaces on EN24 Base Substrate. *International Journal of Mining, Metallurgy & Mechanical Engineering (IJMMME) Volume 1*, 160.

Krastev, D. (2012). Improvement of Corrosion Resistance of Steel by Surface Modification. In D. Shih, *Corrosion Resistance* (pp. 301-303). Bulgaria: In Tech.

Sampath, S. (2015). Thermal spray application in functional material, elecronic and sensors. *Center for Themal Spray Research at Stony Brook University*, 23-26.

Suwattananont, N. (2004). *Surface Treatment of Ferrous Alloys with Boron.* New Jersey: New Jersey Institute of Technology.

Swapp, S. (2011, June 03). *Scanning Electron Microscopy (SEM)*. Retrieved October 11, 2016, from Geochemical Instrumentation and Analysis: http://serc.carleton.edu/research_education/geochemsheets/techniques/SEM.html

Topuz ,P., Cicek ,B., Akar ,O. (2015). Kinetic Investigation of AISI 304 Stainless Steel Boronized in INdirect Heated Fluidized Bed Furnace. *Journal of Mining and Metallurgy*, 64.

Tsipas, D, N & Rus, J. (1987). Boronizing of Alloy Steels. *Journal of Material Science*, 118-120.

Yorulmaz, M. (2007). *An Investigation of Boriding of Medium Carbon Steels.* Istanbul: Marmara Univerdity.

Yu, L.G., Khor, K.A., & Sundararajan, G. (2002). Boriding of Mild Steel using the Spark Plasma Sintering (SPS) Technique. *Surface and Coatings Technology*, 226-230.

APPENDIX A

Cutting process

<u>Molding process</u>

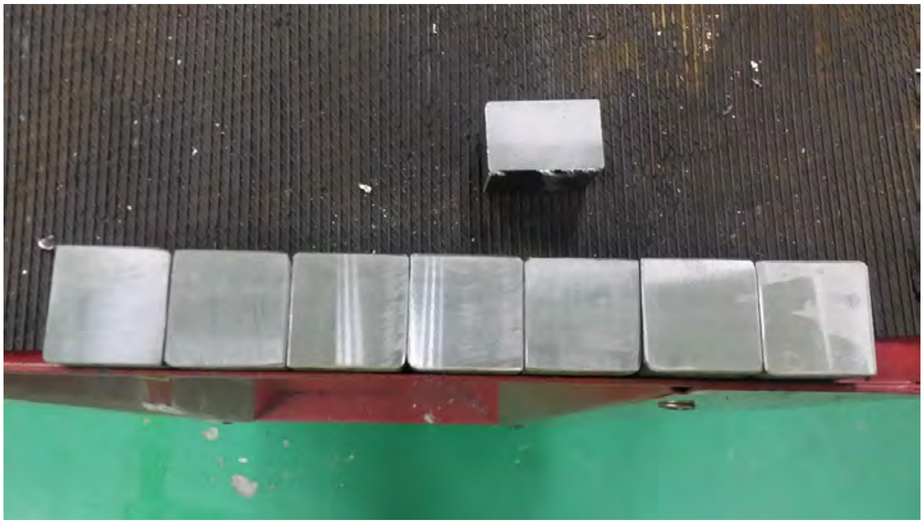

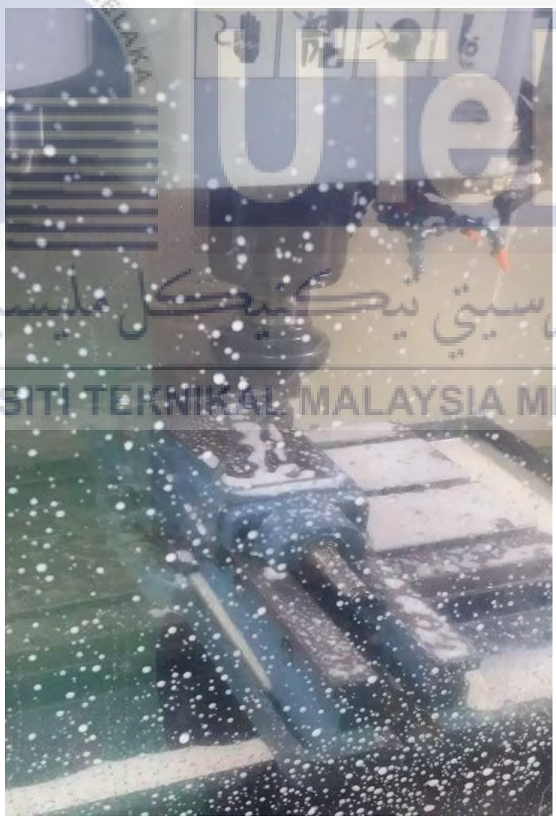


WARNING!

APPENDIX B

Furnace (heating process)

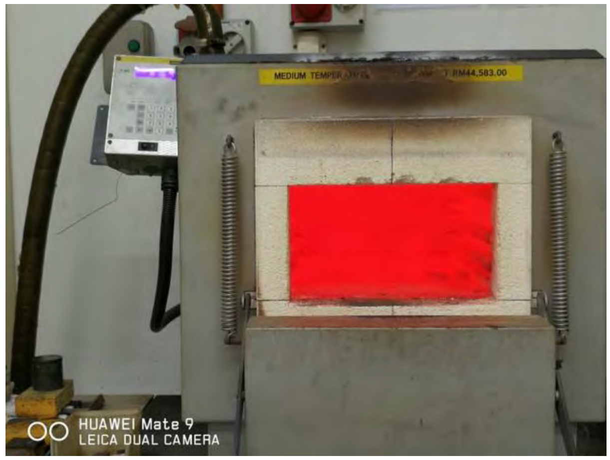

Grind and polish process

APPENDIX C

Measurement of boride layer thickness (SEM)

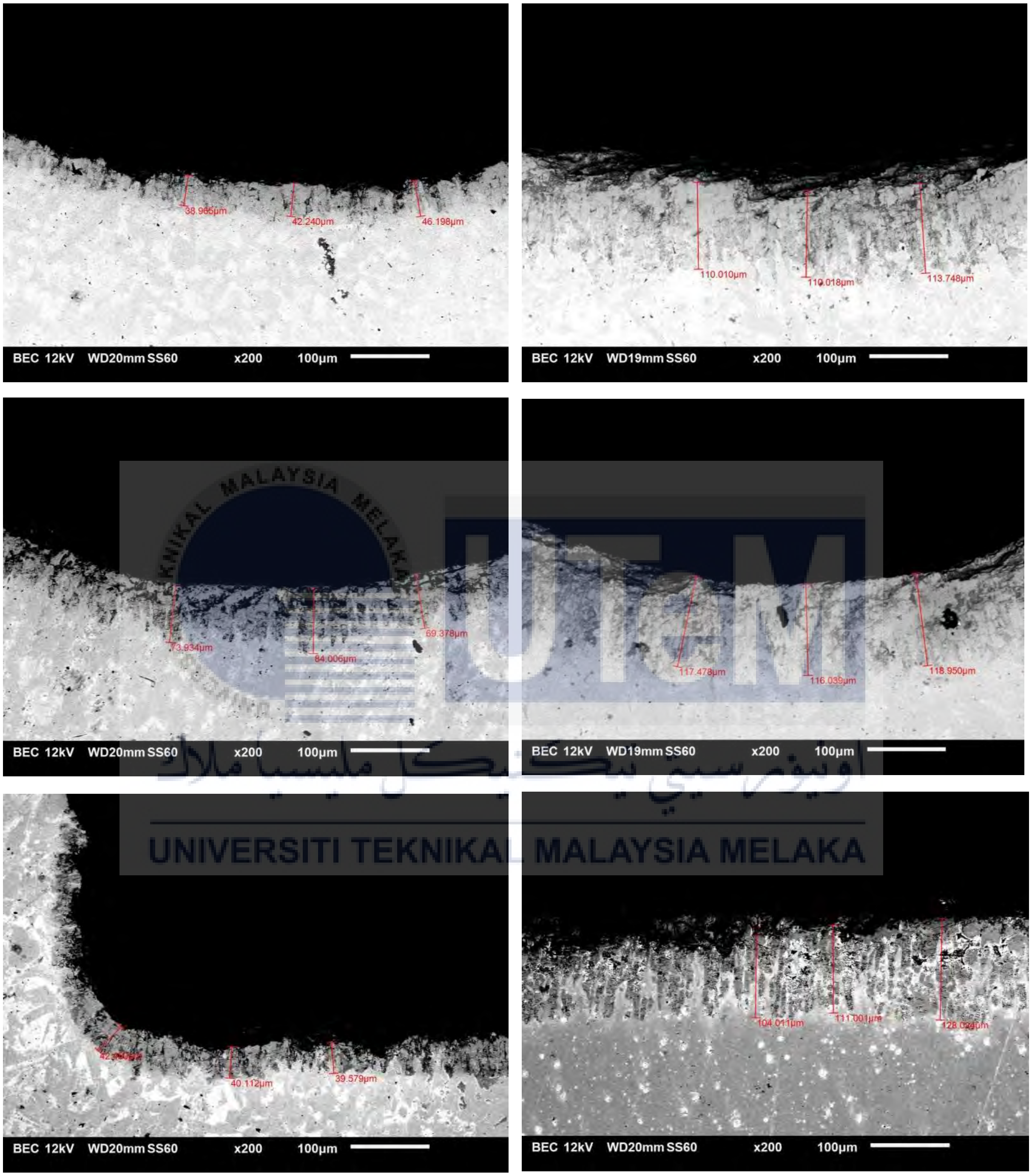

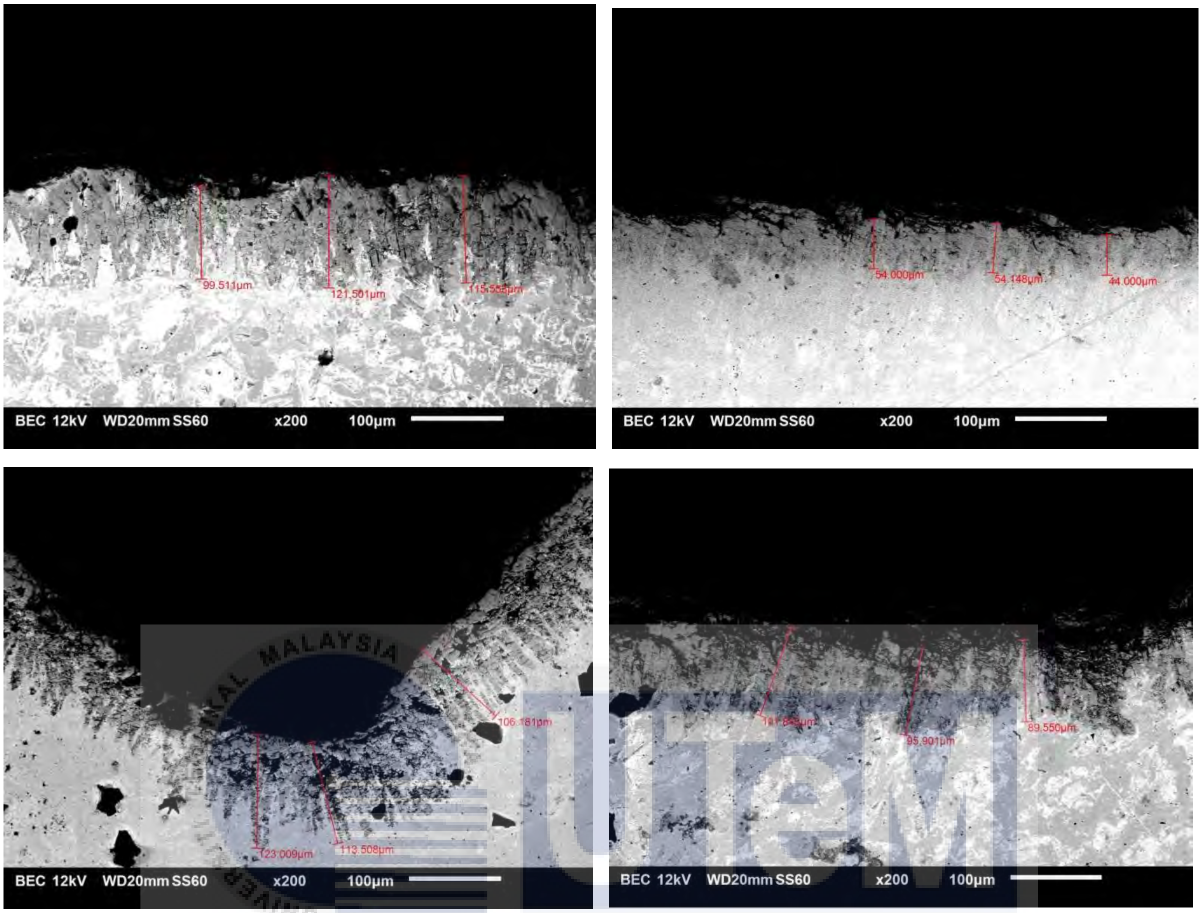
BEC 12kV WD20mm SS60 x200 100µm
99.511µm
121.501µm
BEC 12kV WD20mm SS60 x200 100µm
54.000µm
54.148µm
44.000µm
BEC 12kV WD20mm SS60 x200 100µm
106.181µm
123.009µm
112.508µm
BEC 12kV WD20mm SS60 x200 100µm
95.901µm
89.550µm